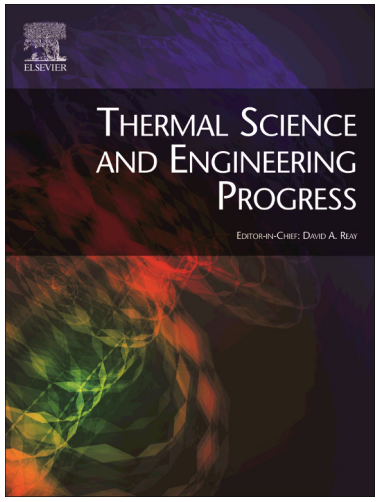

A numerical methodology for comprehensive assessment of the dynamic thermal performance of horizontal ground heat exchangers

Guohui Gan

PII: S2451-9049(18)30559-6
DOI: https://doi.org/10.1016/j.tsep.2019.04.013
Reference: TSEP 349

To appear in: *Thermal Science and Engineering Progress*

Received Date: 28 September 2018
Revised Date: 4 March 2019
Accepted Date: 24 April 2019

Please cite this article as: G. Gan, A numerical methodology for comprehensive assessment of the dynamic thermal performance of horizontal ground heat exchangers, *Thermal Science and Engineering Progress* (2019), doi: https://doi.org/10.1016/j.tsep.2019.04.013

A numerical methodology for comprehensive assessment of the dynamic thermal performance of horizontal ground heat exchangers

Guohui Gan
Department of Architecture and Built Environment, University of Nottingham, University Park, Nottingham NG7 2RD, UK
Email: guohui.gan@nottingham.ac.uk; Tel. +44 115 9514876

Declarations of interest: none

ABSTRACT

Heat transfer takes place simultaneously with moisture transfer in unsaturated soil and the transport processes interact with a ground heat exchanger (GHX) installed for a ground source heat pump. This paper presents a numerical methodology to produce spatiotemporally varying soil properties and assess their interactions with a horizontal GHX and the impacts on its dynamic performance. First, moisture and temperature profiles are generated from the numerical solution of coupled one-dimensional heat and moisture transfer equations and using soil properties that vary with time and depth. Next, governing equations for a three-dimensional mathematical model are solved numerically for a system of atmosphere, soil and horizontally coupled GHX. The model is then used to assess the thermal performance of the GHX under different atmospheric conditions at five installation depths in five soil types. Results demonstrate the importance of coupling moisture transfer with heat transfer in a mathematical model for dynamic thermal simulation of heat exchangers in shallow ground. The atmospheric conditions have been shown to have significant impacts on the dynamic performance which cannot be predicted using a model for heat transfer only. The heat transfer rate of a horizontal GHX varies with time and the depth of installation and the total amount of heat transfer for an operating season increases with installation depth. Heat transfer in moist sandy soil is found to be higher than that in loamy sand soil and much higher than that in loam, clay loam or clay soil.

KEYWORDS: Heat transfer; moisture transfer; horizontal ground heat exchanger; thermal performance; thermal conductivity, soil texture.

NOMENCLATURE

C soil specific heat (J/kgK)

D damping depth of temperature fluctuation (m)

$D_{T,l}$ thermal liquid moisture diffusivity (m^2/sK)

$D_{T,v}$ thermal vapour moisture diffusivity (m^2/sK)

$D_{\Theta,l}$ isothermal liquid moisture diffusivity (m^2/s), $D_{\Theta,l} = K\frac{\partial \psi}{\partial \Theta}$

$D_{\Theta,v}$ isothermal vapour moisture diffusivity (m^2/s)

f ratio of temperature gradient of soil constituent to that of water

GHX ground heat exchanger

GSHP grond source heat pump

HMT heat and moisture transfer

K soil hydraulic conductivity (m/s)

k soil thermal conductivity (W/mK)

L latent heat (J/kg)

q specific heat transfer rate (W/m)

q_v volumetric heat production/dissipation rate (W/m^3)

T soil temperature (^oC)

T_m deep soil temperature (^oC)

T_{amp} amplitude of soil surface temperature variation (^oC)

t time (s or day)

t_o time for occurrence of minimum temperature (day)

Z depth from ground surface (m)

z vertical coordinate (m)

Greek symbols

θ volumetric fraction of a constituent of soil

Θ volumetric moisture content (m^3/m^3)
Θ_i ice (solid moisture) content (m^3/m^3)
Θ_v source/sink of moisture (m^3/m^3s)
ρ soil density (kg/m^3)
ρ_i ice density (kg/m^3)
ρ_l liquid density (kg/m^3)
Ψ matric potential (m)

Subscripts
i ice
l liquid moisture
m m^{th} component of n types of dry soil grains
p pores filled with gas
T thermal
v vapour or volumetric
Θ isothermal

1. INTRODUCTION

A well designed and operated ground source heat pump (GSHP) is able to deliver energy-efficient heating and cooling for a building. However, currently deploying a GSHP system is costly compared with traditional heating and cooling systems. The most expensive part of a GSHP system is the ground heat exchanger (GHX) and its installation. There are two types of GHX in terms of installation direction - horizontal and vertical heat exchangers. Vertical GHX are often installed to depths of 70 to 130 m [1] and they are more widely used because less land is required for their installation. Their wide applications have been accompanied with extensive research on the performance by means of experiments [2-3] and an analytical solution or semi-analytical solution in combination with a numerical method to calculate or compare g-functions [4-6]. Installation of a vertical GHX requires specialised equipment which makes it much more expensive than the heat pump of the system. By comparison, a horizontal GHX can be installed in shallow ground typically 1 – 2 m deep with the help of an excavator and so is cheaper to install but requires more land for the installation to obtain the same amount of heat transfer. Another feature of a horizontal GHX is that its performance is less predictable because of larger spatial and temporal variations in the soil temperature and moisture as well as thermophysical properties in shallower ground.

This work is concerned with the horizontal type of GHX. The main part of most horizontal GHXs consists of either simple straight pipes or geometrically complicated slinky coils. Similar to the vertical GHXs, horizontal GHXs have also been investigated for GSHPs experimentally, mathematically or numerically. Earlier experimental work on GSHPs involved mainly straight pipes. Demir, et al. [7] measured the performance of a GSHP with three 40 m long parallel pipes buried 1.8 m deep whereas Esen, et al. [8] used a single pass pipe of 50 m long and buried 1 m deep. More recent experiments on horizontal GHXs have been mostly focused on a slinky type that is able to extract more heat per unit area of installation than straight pipes for short term or intermittent operation. Wu, et al. [9] measured the thermal performance of slinky coils installed in an area of 80 m long and 20 m wide and about 1.2 m deep. Fujii, et al. [10] tested three slinky coils that have a loop diameter of 0.8 m but have three different pitches of 0.4, 0.6 and 0.8 m, each installed at 1.5 m deep in an area of 35 m long and 4 m wide. Esen and Yuksel [11] experimentally evaluated a 150 m long slinky heat exchanger installed in a channel of 15 m long and 2 m deep for heating of a greenhouse. Adamovsky, et al. [12] measured the changes in energy and temperature in the

ground with both straight and slinky heat exchangers. The straight heat exchanger with a total length of 330 m was installed at 1.8 m deep and with a 1 m span whereas the slinky heat exchanger with a total length of 200 m was installed at 1.5 m deep in 53 loops with a 0.38 m pitch. The thermal properties of dry soil are usually poorer than those of wet soil. Platts, et al. [13] developed a concept to enhance the thermal properties of dry soil whereby an impervious membrane was used to enclose a volume of soil surrounding a heat exchanger and the soil was then artificially wetted. Experimental and numerical tests were conducted to validate the concept for a 16 m long straight heat exchanger installed at 2 m deep.

The results of laboratory or field experiments on a horizontal GHX are valuable not only for assessing its performance but also for validating a computer model. However, on the one hand, because of the interactions of the GHX with varying atmospheric conditions and surrounding soil whose range of influence expands with time, field testing is required for determining the long-term performance as laboratory testing in a confined space would not be able to simulate such real environmental conditions. On the other hand, field measurements often include the output of a GHX in terms of the flow rate and temperature change of the working fluid but not spatiotemporally varying soil properties during operation or even before installation at the design stage. Hence, such measured results are unique for the system in consideration and would not be fully transferable for design and performance assessment of systems installed in soil with different properties or in a different climate. One solution to such a problem is mathematical modelling. Valid mathematical models enable performance prediction with more details of transport processes involved and design optimisation for a GHX and the system. Again as for a vertical GHX, an analytical one-dimensional heat transfer model may be used for horizontal straight GHXs in soil of homogeneous properties. It is even possible to obtain analytical solutions for a GHX with a complicated geometry. For example, Li, et al. [14] developed analytical solutions for a horizontal spiral heat exchanger in both infinite and semi-infinite soil of uniform and constant properties, at a uniform initial temperature and under a constant surface temperature or an adiabatic boundary condition. For complex heat transfer processes such as those involving interactions between soil, atmosphere and the GHX, however, a numerical method is required for the solution.

Besides, not only the temperature but also moisture content in shallow ground vary significantly in space and time and their variations are interdependent. Measurements by Nayler, et al [15] at three depths of 1.2 m, 1.5 m and 1.8 m in the Midwestern USA confirmed large variations in soil properties as a result of moisture fluctuations and consequently unsaturated soil would be inhomogeneous for heat transfer. Hence, both heat and moisture transfer (HMT) equations have to be solved numerically for a horizontal GHX in inhomogeneous soil. Numerical solutions of coupled HMT equations have so far enabled a wide range of predictions from food processing [16-17], the indoor thermal environment [18], soil deformation [19], moisture evaporation from soil [20] to temperature and moisture variations of soil alone [21-23] or buried with a GHX [24-26].

The solution accuracy for transient HMT in shallow ground depends on the reliable initial thermosphysical properties of soil and its temperature and moisture in addition to the appropriate model equations, numerical method and boundary conditions. For soil with homogeneous properties, the initial soil temperature may be taken as the following commonly used analytical equation for sinusoidal temperature variation with depth at a time corresponding with the start of system operation,

$$T = T_m - T_{amp} e^{-Z/D} \sin\left((t - t_0)\frac{2\pi}{365} - \frac{Z}{D} - \frac{\pi}{2}\right) \quad (1)$$

For real soil with spatially and temporally varying moisture and thermophysical properties, such an analytical equation may not be adequate to represent the temperature variation. It has been shown that significant errors in soil temperature between this type of analytical equation and real measurements would occur – as much as 10% to 15% based on the magnitude of annual variation and nearly 50% based on the daily mean variation [27]. To provide a more realistic representation of soil temperature, Droulia, et al. [28] developed a semi-empirical model for estimating the ground temperature by replacing the annual mean soil surface temperature in the analytical equation with observed daily mean soil temperatures at different depths. Based on the observed weather data for Hong Kong, Chow, et al. [29] developed a multivariable regression model for predicting the soil temperature from given air temperature. The model was site specific but applicable for the city of Hong Kong due to similar soil conditions. Chalhoub, et al. [23] developed a simple HMT model to predict the soil temperature. The model took into consideration of spatiotemporal-varying heat and mass balances at the soil surface and soil temperature but the bulk soil was divided into two layers only for the calculation of soil moisture and thermophysical properties.

Unlike Equation (1) for temperature variation in homogeneous soil, such a simple expression is not available for soil moisture variation. To obtain a moisture profile requires numerical integration of transient water flow equations in soil. The numerical solution of either moisture transfer alone or more generally coupled with heat transfer requires the initial data for soil moisture. The initial soil moisture may be taken to be uniform but this is unlikely realistic in unsaturated soil. A more accurate approach for initialisation of soil moisture is to make use of the solution of Richards equation [30] for a known depth of water table but it is not ideal either. Firstly, the depth of water table varies considerably with location and season and so it is not feasible to use the solution for a generic unspecific site. Secondly, moisture variation profiles differ considerably for different water table depths as illustrated in Fig. 1 which is obtained from the solution of Equation (9) for loam soil. Thirdly, this type of profile may not hold all the time because it does not include the influence of temporal variations in ambient and soil conditions or moisture sources and sinks such as moisture injection by precipitation or irrigation and extraction by plant roots. In fact, depending on the climatic conditions, soil moisture near the surface in part of the UK could be higher for most of the time of a year [31] rather than increasing with depth from lower at the surface as predicted from the equation. Therefore, to acquire realistic ground temperature and moisture variations should be an indispensable part of a comprehensive model for a horizontal GHX.

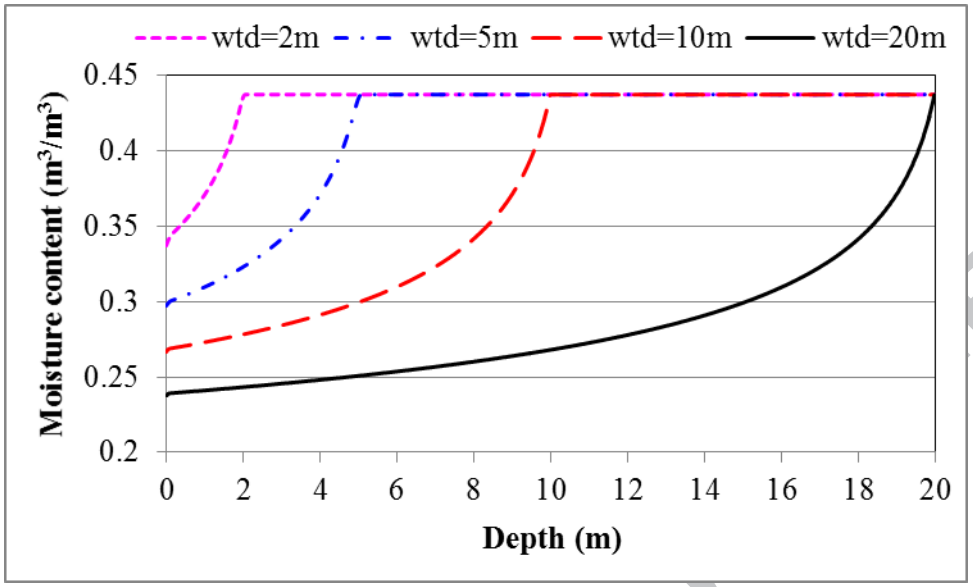

Fig. 1 Vertical moisture profiles in loam soil for different water table depths (wtd)

The main objective of the present work is to develop a comprehensive numerical methodology for dynamic thermal simulation of horizontal GHXs. The methodology takes account of coupled HMT in soil before and during operation and interactions of the GHX with soil and atmosphere. Initial data profiles are first generated which account for spatiotemporal variations in soil properties. The seasonal performance of the GHX is then predicted using the model with coupled HMT. Another objective is to demonstrate the importance of taking full account of moisture transfer through comparison of the predicted results between the coupled HMT model and a heat transfer model without consideration of moisture transfer.

2. METHODOLOGY

The performance of a horizontally coupled GHX is predicted with numerical solution of equations for transient HMT in soil in combination with expressions for soil properties that vary with time and depth. The solution of the equations requires i) spatially varying initial soil properties and conditions and ii) temporally varying boundary conditions.

2.1 Model equations

The mathematical model describing the spatial and temporal variations of soil temperature and moisture is given as follows [32]:

$$\frac{\partial(\rho CT)}{\partial t} - L_i\frac{\partial(\rho_i \Theta_i)}{\partial t} = \nabla\cdot\left((k + L\rho_l D_{T,v})\nabla T\right) + \nabla\cdot(L\rho_l D_{\Theta,v}\nabla\Theta) + q_v \tag{2}$$

$$\frac{\partial\Theta}{\partial t} = \nabla\cdot\left((D_{T,l} + D_{T,v})\nabla T\right) + \nabla\cdot\left((D_{\Theta,l} + D_{\Theta,v})\nabla\Theta\right) + \frac{\partial K}{\partial z} + \Theta_v \tag{3}$$

During heat extraction, there is a possibility that moisture could condense on the external pipe surface and this would form a source of moisture (Θ_v) and an associated heat source (q_v) due to the condensation and likewise a moisture and heat sink due to consequent evaporation. There are other potential sources or sinks such as irrigation as a moisture source and moisture extraction by plant roots as a sink, useful for simulation of a specific system of soil, atmosphere and vegetation but neglected for more generic soil conditions in this study.

The second term $L_i\frac{\partial(\rho_i\Theta_i)}{\partial t}$ in Equation (2) represents the energy for potential soil freezing or thawing near the surface of the ground and/or GHX for winter heating operation. If evolution of the freezing/thawing process is not a concern, the term can be moved to the right side and combined with the source/sink for heat transfer, i.e.

$$\frac{\partial(\rho CT)}{\partial t} = \nabla\cdot\left(\left(k + L\rho_l D_{T,v}\right)\nabla T\right) + \nabla\cdot\left(L\rho_l D_{\Theta,v}\nabla\Theta\right) + q_v \tag{2a}$$

The thermophysical properties of soil are calculated using the following equations:

$$\rho = \sum_{m=1}^{n}\rho_m\theta_m + \rho_l\theta_l + \rho_i\theta_i + \rho_p\theta_p \tag{4}$$

$$C = \frac{\sum_{m=1}^{n}\rho_m C_m\theta_m + \rho_l C_l\theta_l + \rho_i C_i\theta_i + \rho_p C_p\theta_p}{\sum_{m=1}^{n}\rho_m\theta_m + \rho_l\theta_l + \rho_i\theta_i + \rho_p\theta_p} \tag{5}$$

$$k = \frac{\sum_{m=1}^{n}f_m k_m\theta_m + k_l\theta_l + f_i k_i\theta_i + f_p k_p\theta_p}{\sum_{m=1}^{n}f_m\theta_m + \theta_l + f_i\theta_i + f_p\theta_p} \tag{6}$$

2.2 Boundary conditions

A large rectangular computational domain is used for simulation. The domain is filled with soil and a horizontal GHX consisting of a number of straight parallel pipes installed in the soil at a certain depth. The length and width of the domain depends on the size of the GHX and the depth is 10 m but could be more for generating initial temperature and moisture profiles for deeper water tables as presented in Fig. 1, Fig. 3 to Fig. 9. The boundary conditions are specified on six faces of the rectangular domain and four surfaces of each circular pipe (inner and outer cylinders, inlet and outlet openings). The boundary conditions are illustrated in Fig. 2. The top surface boundary involves all modes of HMT and their coupling including i) condensation, evaporation, freezing, thawing, precipitation and diffusion for moisture transfer and ii) wind- and buoyancy-induced natural convection, short and long wave radiation and heat conversion from precipitation, evaporation/condensation and freezing/ thawing as well as conduction heat transfer through the ground surface. These processes require the input of the time-dependent atmospheric conditions including air temperature and humidity or vapour pressure, solar radiation, wind speed, cloud cover and precipitation. Details of the boundary conditions can be found in references [25, 33].

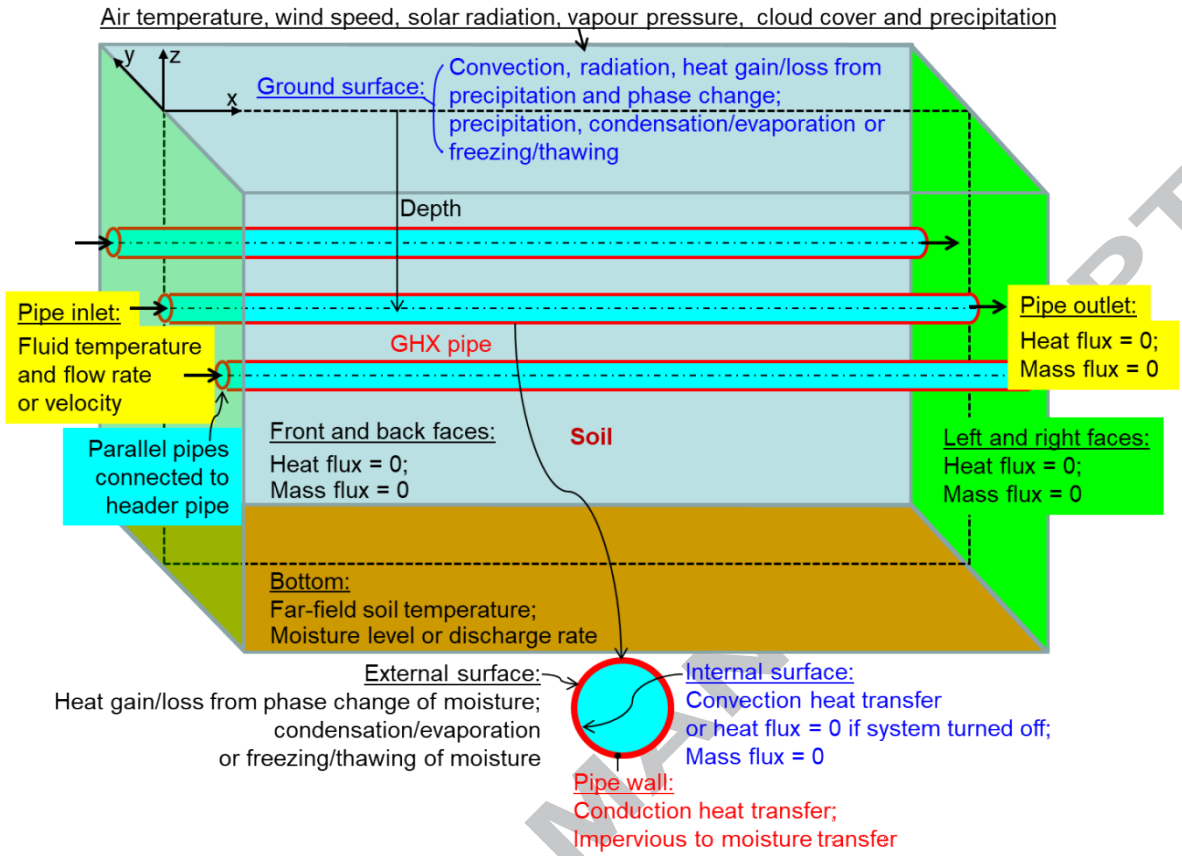

Fig. 2 Boundary conditions for simulation of coupled HMT

2.3 Initial conditions

The main initial soil conditions for simulation are soil temperature and moisture. Since soil temperature and moisture are not uniform in soil, their vertically varying profiles are produced for initialisation. The profiles take account of temporal variations in ambient conditions and soil properties that are in turn influenced by the temperature and moisture. To speed up the process, equations (2a) and (3) are simplified to the following one-dimensional equations for vertical HMT without a GHX:

$$\frac{\partial(\rho CT)}{\partial t} = \frac{\partial}{\partial z}\left(\left(k + L\rho_l D_{T,v}\right)\frac{\partial T}{\partial z}\right) + \frac{\partial}{\partial z}\left(L\rho_l D_{\Theta,v}\frac{\partial \Theta}{\partial z}\right) + q_v \quad (7)$$

$$\frac{\partial \Theta}{\partial t} = \frac{\partial}{\partial z}\left(\left(D_{T,l} + D_{T,v}\right)\frac{\partial T}{\partial z}\right) + \frac{\partial}{\partial z}\left(\left(D_{\Theta,l} + D_{\Theta,v}\right)\frac{\partial \Theta}{\partial z}\right) + \frac{\partial K}{\partial z} \quad (8)$$

Equations (7) and (8) are solved using the control volume method (described in Section 2.4) continuously for at least two years. Simulation starts from the instant when the system is supposed to start operating, eg, the 1st of October for heating. Results between two consecutive years are then compared and if their differences in the soil temperature and moisture at any depth are negligible, the final set of data is taken as the initial values.

The solution makes use of the same conditions as above for the top surface boundary in Fig. 2. For moisture at the bottom boundary, any known condition can be used such as a moisture (water) discharge rate. Here, two types of bottom boundary condition - zero mass flux and fixed saturation moisture - and two types of initial soil moisture (uniform or varying with depth to a water table depth) are used. The varying initial moisture is given by the following Richards equation which can be derived from Equation (8) for isothermal water flow in unsaturated soil:

$$\frac{\partial \Theta}{\partial t} = \frac{\partial}{\partial z}\left(K\left(\frac{\partial \Psi}{\partial z} + 1\right)\right) \tag{9}$$

Equation (9) can be solved numerically in general. However, it is possible to solve the equation analytically for homogeneous or layered soil under special initial and boundary conditions [34]. Fig. 3 shows the numerically predicted variation of moisture (wetting) profiles in loam soil with a bare soil surface for different months from initial settings (with a fixed water table depth of 20 m) at a site in Southern England. It can be seen that the profile below 2 m is well established after three months with nearly a uniform moisture level up to about 2.5 m from the bottom. Monthly variation from the soil surface to 2 m deep is however considerable due to varying atmospheric conditions. Similarly diurnal variation would be significant nearer the surface. For this range of depth, the soil moisture generally increases with depth unless it rains when the soil surface would be saturated and the moisture decreases with the increase in depth up to 0.67 m (see an example shown in Fig. 15).

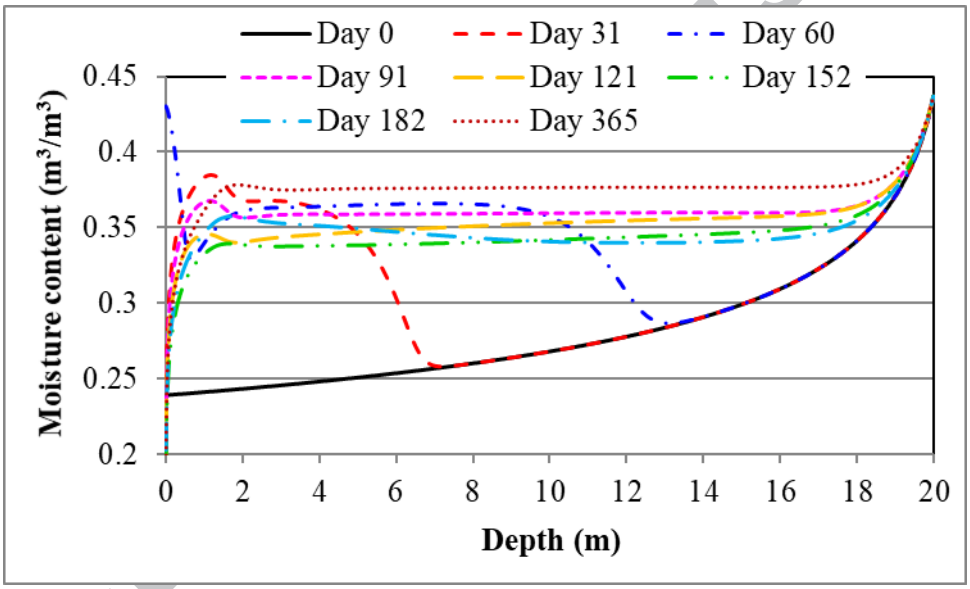

Fig. 3 Predicted variation of moisture profile from initial setting

From a comparison of the moisture profiles between two consecutive years presented in Fig. 4(a) and Fig. 3 for a water table depth of 20 m, it turns out that for all practical purposes, such an initial setting would have already been transformed into a moisture profile for a type of soil under a set of time-varying climatic conditions after three months, with a maximum difference of less than 1% for the entire depth as shown in Fig. 4(b), and results from then on can be used for initialisation for any starting time. This means that, eg, if a simulation is performed for a heating season starting from October, the initial moisture profile could be established through modelling of one-dimensional transport phenomena from July or earlier. In Fig. 4(a), the data line for Day 365 (end of the 2nd year) completely overlaps that for Day 0 (end of the 1st year).

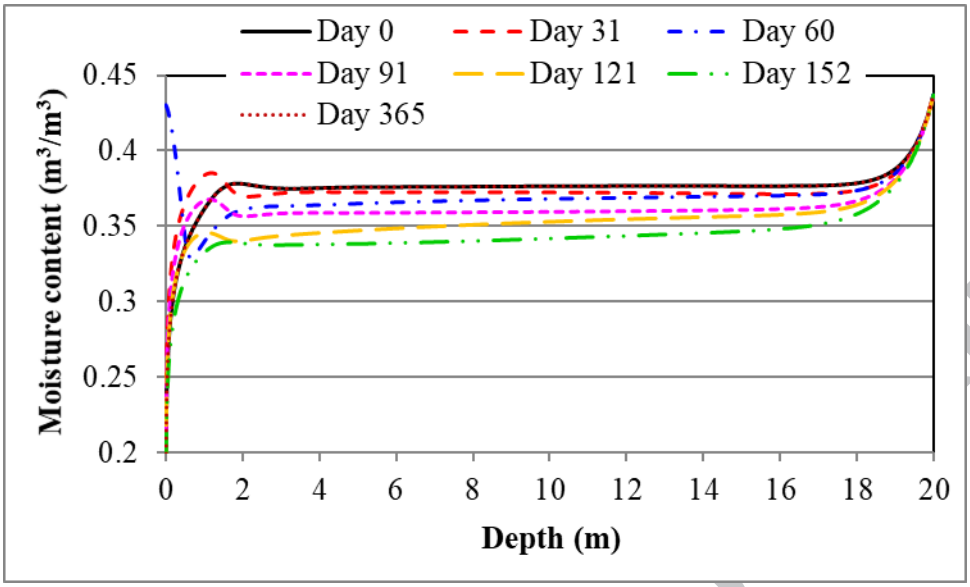

(a) Predicted variation of moisture profile for the 2nd year

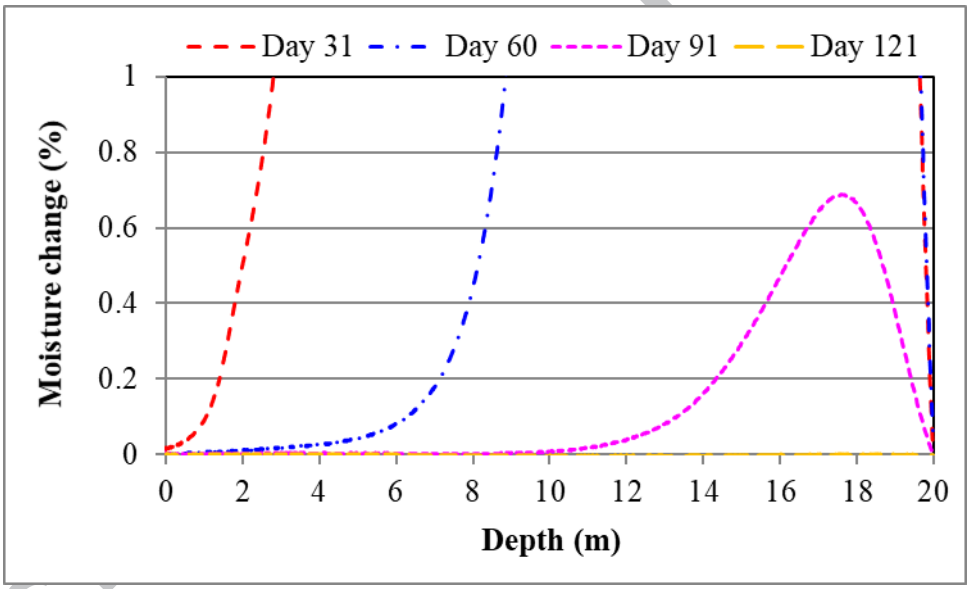

(b) Change between the 1st and 2nd years

Fig. 4 Predicted moisture profiles for the 2nd year and changes from the 1st year

The depth of water table in Equation (9) has been found to have hardly any effect on the final moisture profile in loam soil for initialisation so long as the intended depth of water table for simulation is kept the same. That is, any depth (eg 5 m) of water table can be used in Equation (9) to calculate the initial moisture data for the solution of Equations (7) and (8) which may have a different depth (eg 20 m) as specified. The predicted moisture profiles are compared in Fig. 5 at different times of the first year between initial water table depths of 5 m and 20 m. The profiles for 20 m initial water table depth are discussed earlier as shown in Fig. 3. It is seen that Fig. 5(b) resembles very much Fig. 4(b) even though the two figures are for different comparisons – one for the same water table depth between two years and another for two water table depths for the same (first) year. Again, there is little difference in the moisture profiles after three months for different initial water table depths (but with saturation at the same depth in the end). Results for the fourth month and forward are exactly

the same for different initial water table depths or profiles as long as the bottom boundary is given the same moisture content, eg saturation moisture.

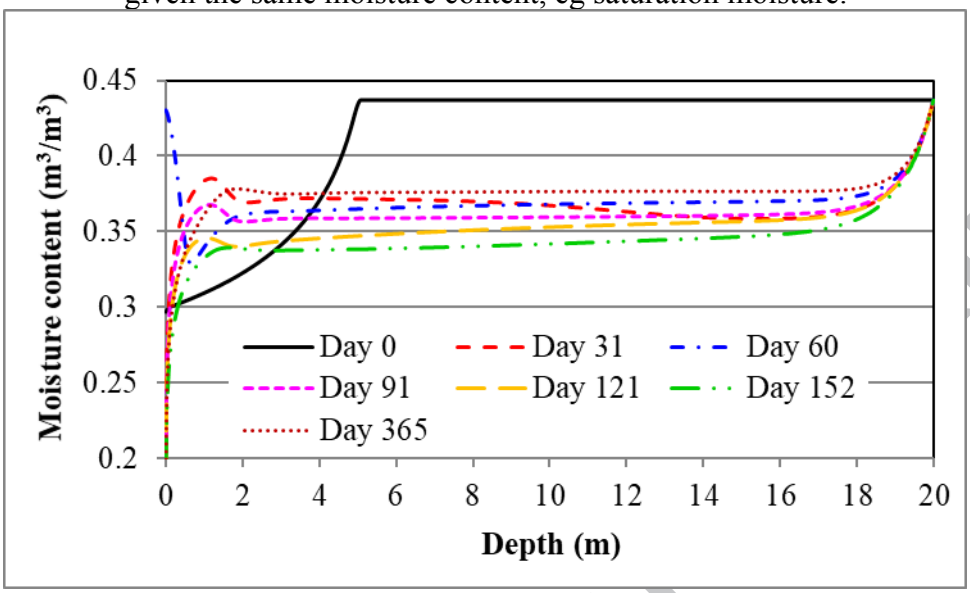

(a) Predicted variation of moisture profile with 5 m initial water table depth

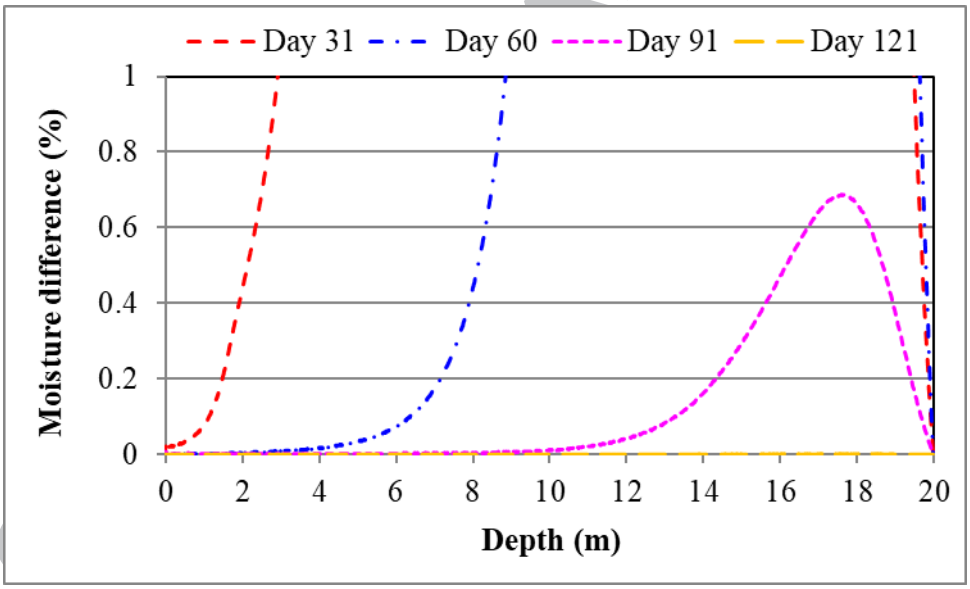

(b) Difference between 5 m and 20 m depths of initial water table

Fig. 5 Effect of initial water table depth on the predicted moisture profiles

Besides, a uniform initial moisture value is used to derive the moisture profile for comparison. Figure 6 shows the predicted soil moisture with a saturation moisture at the bottom boundary and a uniform initial moisture (= one half of the saturation moisture content) for the whole domain. The predicted difference using the uniform and varying initial moisture conditions is less than 1% from the soil surface to the water table depth after four months and the whole profile would become almost identical to that in Fig. 3 after five months. Hence, one apparent advantage of Equation (9) over a low uniform value for initialisation is the reduction of the period required for calculation from initial values towards final results by about one month. However, this advantage would diminish if a higher uniform moisture content is used for initialisation. For example, when the uniform initial moisture value is increased to ¾ of the saturation moisture content, it would only require a

calculation for three months to achieve a maximum difference of less than 1% for the whole domain and this is shown in Fig. 6 as Day 91_75%.

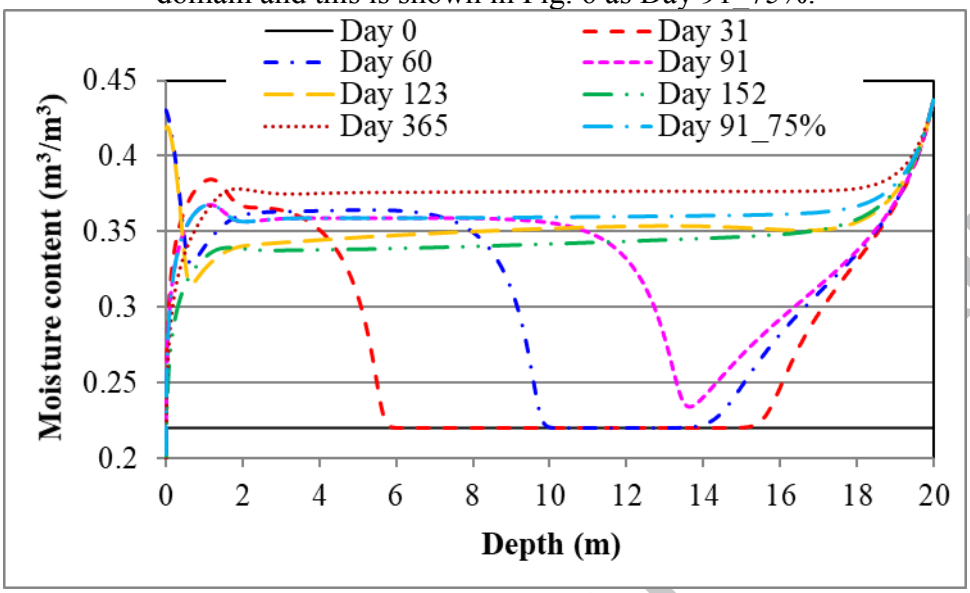

(a) Predicted variation of moisture with a uniform initial value and a saturation value at bottom

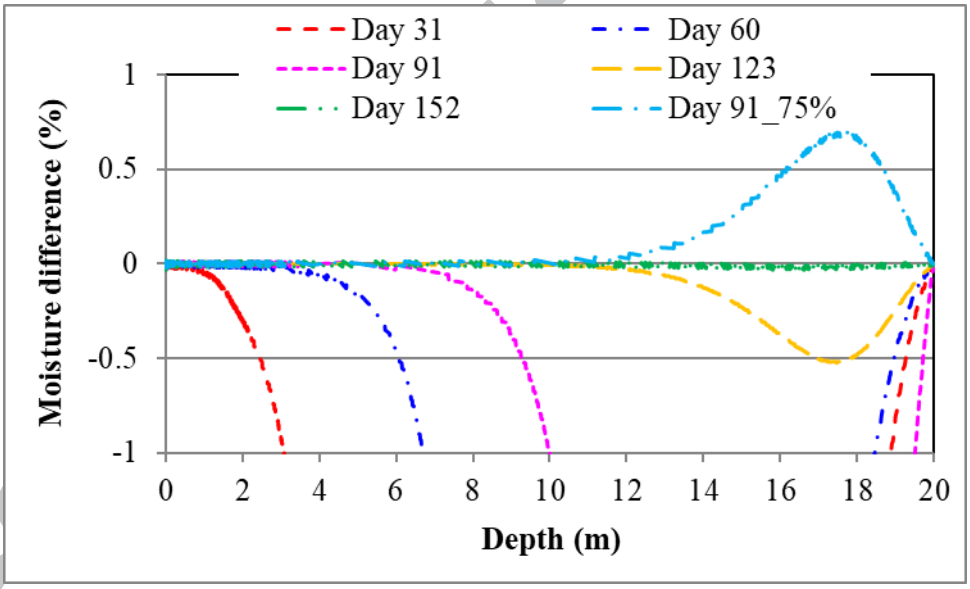

(b) Difference between initially uniform value and varying with depth

Fig. 6 Effect of initial moisture setting on the predicted moisture profile

Even with a uniform initial value and zero moisture transfer at the 20 m bottom boundary, the difference would be below 1% up to 16 m deep after six months and to 18.4 m at the end of one year as shown in Fig. 7. However, assuming zero moisture flux at the bottom boundary means that the moisture would not be able to reach the saturation moisture content under the given conditions and thus the difference between Fig. 7(a) and Fig 3 would remain large close to the bottom; eg, the difference after one year is still much larger than 1% for 1.6 m distance from the water table as shown in Fig. 7(b). The purpose of this prediction is simply to show that the effect of the initial moisture content is negligible for the final results away from the area near the water table. Of course, the difference can be eliminated for the entire domain if the same boundary conditions are used, as illustrated for Fig. 6.

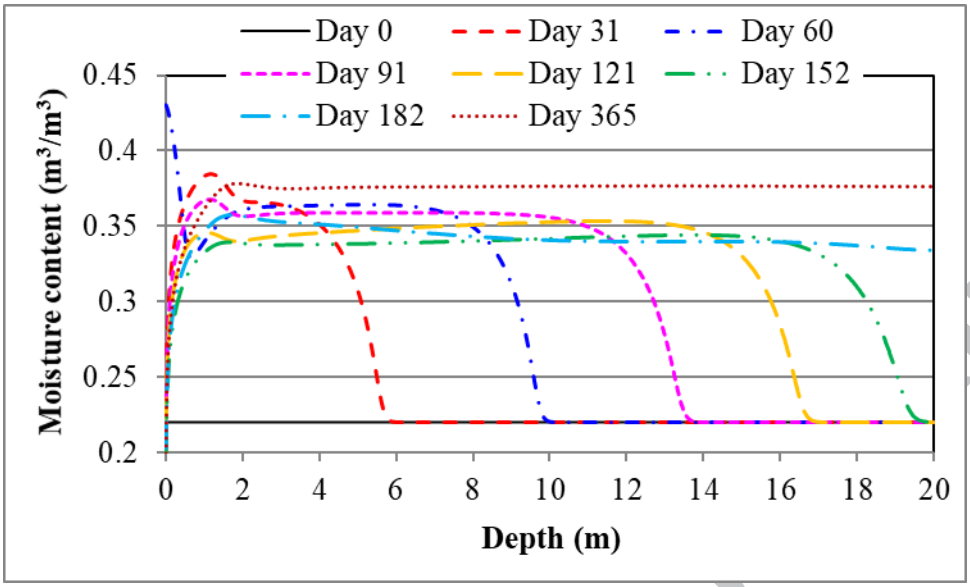

(a) Predicted variation of moisture with a uniform initial value and zero moisture flux at bottom

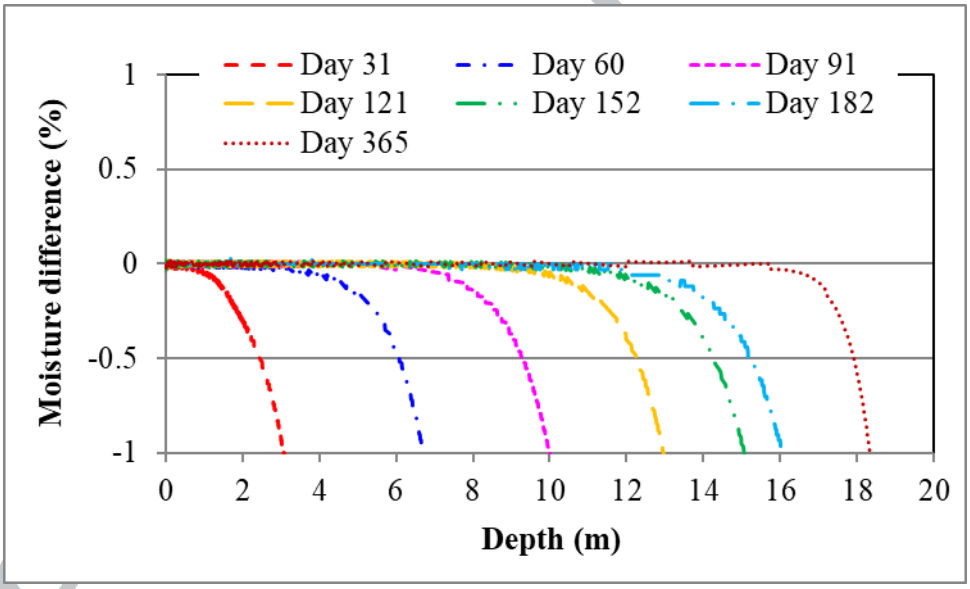

(b) Difference from initially varying moisture with depth

Fig. 7 Effect of initial and boundary conditions on the predicted moisture profiles

An added benefit of the solution of Equations (7) and (8) is a new vertical soil temperature profile which can be used for initialisation. This type of temperature profile is more realistic because it accounts for varying ambient and soil conditions. However, it would take a longer time to generate a temperature profile than that for the moisture profile, depending on the type of the initial and boundary conditions employed for the bottom point. Assuming that the initial temperature is given by Equation (1) with the deep soil temperature taken to be the annual mean air temperature, Fig. 8a shows the changes of the temperature between consecutive years where, eg, yr 1/2 represents the relative change from the 1st to the 2nd year. The temperature profiles at the end of the 1st and 5th years (Year 1 and Year 5 respectively) are also presented. It is seen that to generate the vertical temperature profile with zero heat flux as the bottom boundary would require simulation of at least four years' process when the maximum difference between the last two years is below 1% for the whole depth.

Nevertheless, the maximum difference is already less than 1% from the soil surface to 7 m deep after simulation of one year's operation below which a horizontal GHX is unlikely to be installed. However, the cumulative difference would be slightly larger eg between the 5th year and the 2nd year – about 1% at 0.8 m deep and over 2% at 5.3 m deep. It is also seen from the figure that the difference increases slightly towards the bottom from the third year. This is the consequence of assuming the annual mean air temperature as the initial deep soil temperature and zero heat flux at the bottom of the boundary but the heat exchange between atmosphere and soil under such conditions would lead to a net heat gain by deep soil to reach an equilibrium temperature higher than the assumed initial value, since it is known that the deep soil temperature is in general higher than the annual mean air temperature [35]. Hence, the number of years to achieve the required difference could be reduced if the deep soil temperature in Equation (1) for initialisation is set at a higher value than the annual mean air temperature for the site.

Alternatively, if the bottom boundary is a fixed deep soil temperature, eg annual mean air temperature, the difference in the predicted soil temperature between consecutive years would be smaller and consequently a two-year simulation may be sufficient to achieve a maximum difference of less than 1%, as shown in Fig. 8b.

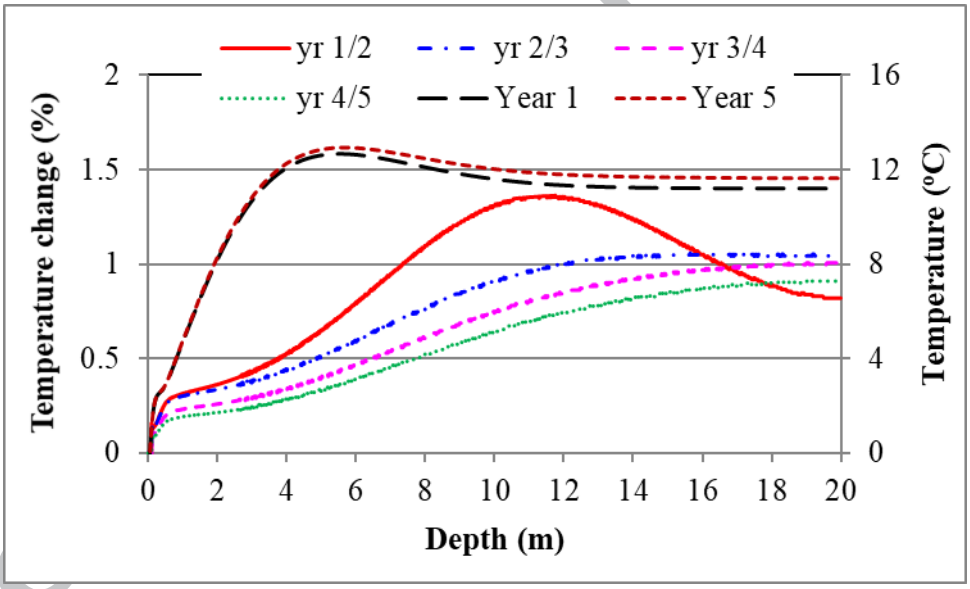

(a) Zero heat flux at the bottom

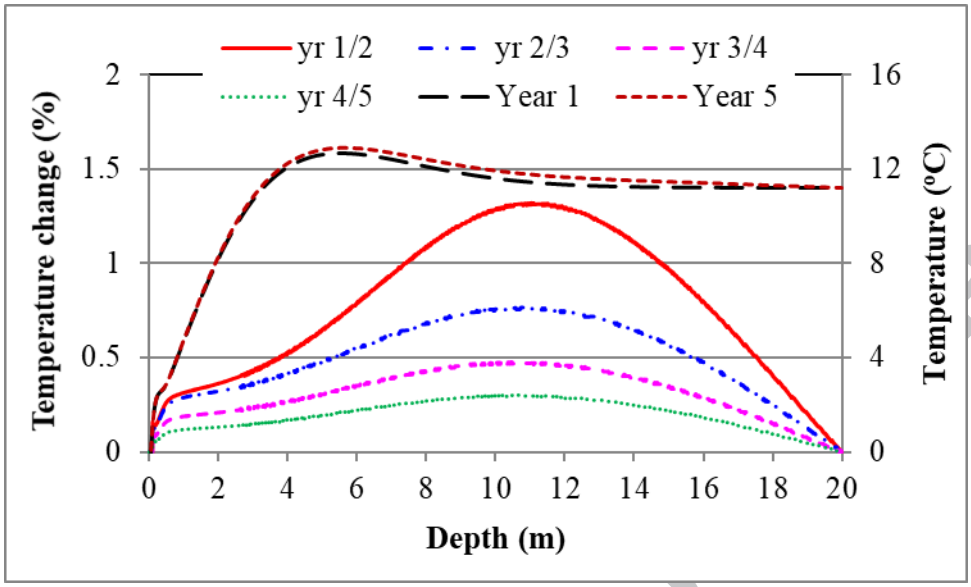

(b) Fixed deep soil temperature

Fig. 8 Predicted temperature profiles and changes between consecutive years

The simulated new temperature profile (in inhomogeneous soil in terms of spatiotemporally varying moisture and associated soil properties) differs from Equation (1) for homogenous soil properties as shown in Fig. 9. The variation in the vertical temperature is larger and extends deeper from the simulation than the analytical equation when the water table is at 20 m deep. The variation according to the analytical equation is limited to a depth of about 10 m but it reaches over 18 m deep from the simulation with a difference of about 4% between 10 m and 18 m at the time. The simulated temperature is lower than that calculated using Equation (1) between the soil surface and about 4 m deep, while it is higher for soil deeper than 4 m, at the beginning of a calendar year. The difference is over 40% from the surface to 1 m deep and over 20% up to 2 m deep. The ground surface temperature at the midnight is below the freezing point from the simulation but could not be predicted with certainty using an analytical equation that is based on an annual temperature profile, although it may be possible to improve the prediction using an analytical equation that includes both annual and diurnal variation of soil temperature.

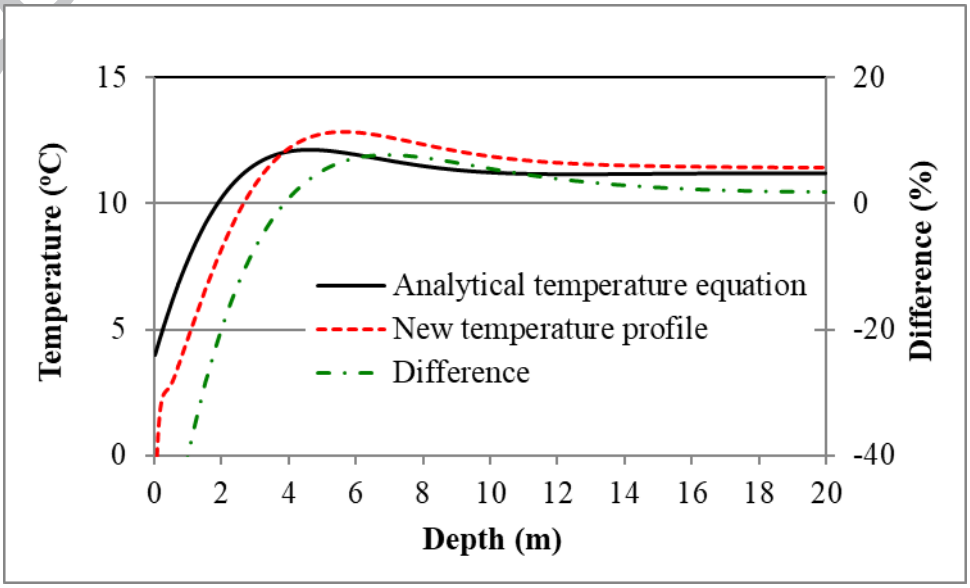

Fig. 9 Difference in temperature profile between homogenous and inhomogeneous soil models at the beginning of a year

2.4 Solution method and simulation procedure

The control volume method is used to solve the model equations together with the initial and boundary conditions. The method involves decomposing a three-dimensional computational domain into numerous small control volumes or cells, integrating each of the partial differential equations over each control volume and then discretising into an algebraic equation. The process is applied to all the cells in the computational domain for numerical solution. An accurate solution of the equations requires careful consideration of the mesh distribution and time steps.

A non-uniform mesh is used for simulation with fine cells distributed in areas with possible large variations in HMT including the heat exchanger and surrounding soil and the vicinity of ground surface. From a grid sensitivity study, it has been found that to obtain an accurate and mesh-independent dynamic thermal simulation requires the edge size of a cell as small as one millimeter in these critical areas. The cell size can then increase gradually away from the areas. Fig. 10 shows an example of the variation of the cell size in the vertical direction with the centre of the heat exchanger pipe at 1.5 m deep.

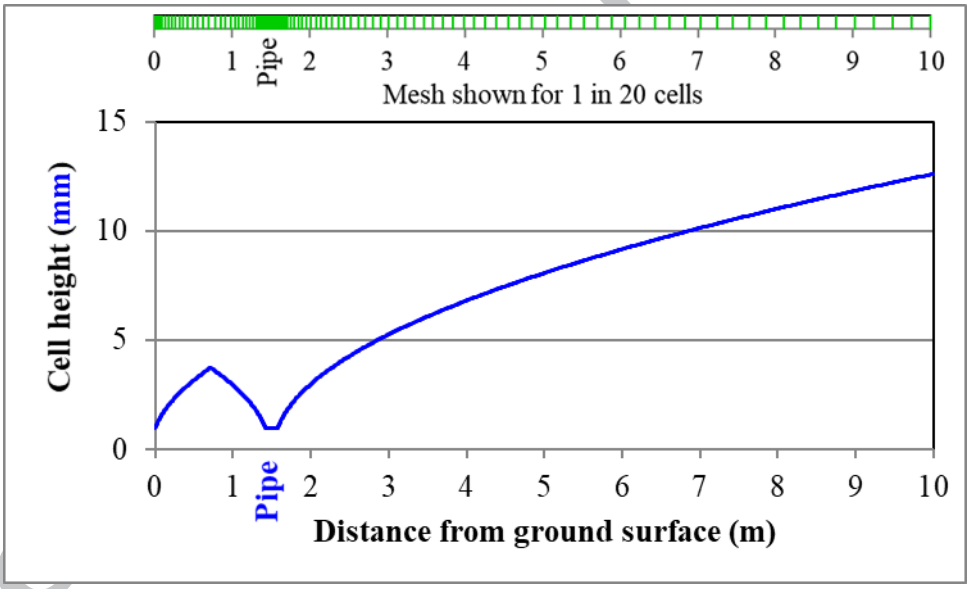

Fig. 10 Cell distribution in vertical direction

Small time steps are used to ensure dynamic simulation is independent of the size of temporal discretisation. The time steps increase gradually from one second at the beginning (for half an hour) of system operation to five minutes after 30 days as shown in Fig. 11. Similar treatment is applied to times when large changes in HMT occur such as the period right after the system is switched on or off for intermittent operation, or during and after intermittent water flow into soil due to rainfall. This means for an intermittent operation of 12-hour on and 12-hour off as an example, only the time steps for the first 12 hours shown in the figure are used, i.e., increasing from one second to a maximum of 60 s for the last two hours of each on or off period.

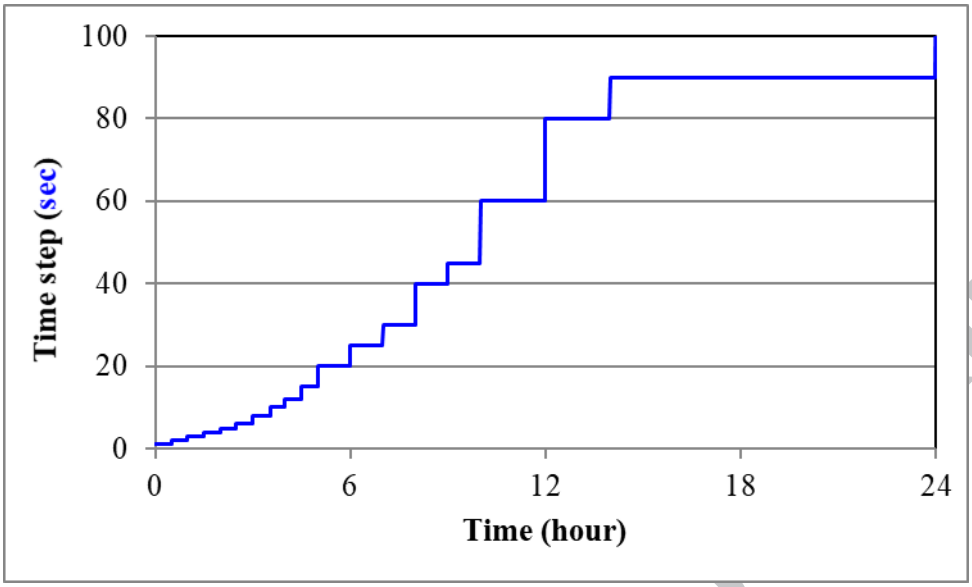

(a) For the first day

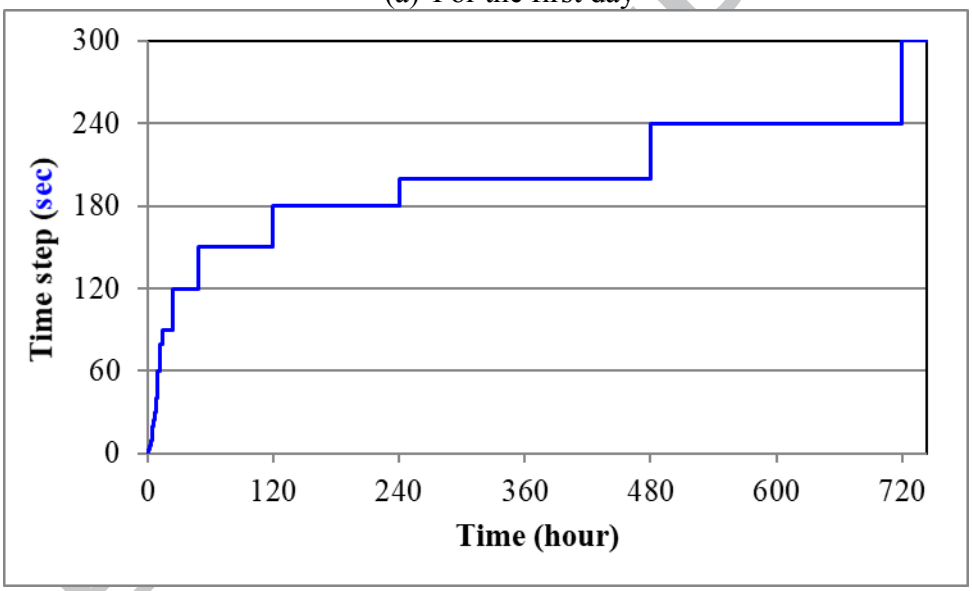

(b) For the first month

Fig. 11 Varying time steps for dynamic simulation

A solution is considered to have converged for each time step when the normalized residual, the sum of the changes between two consecutive iterations in, eg, soil temperature normalized with the magnitude for the computational domain is less than 0.0001 and the change in heat flux through the GHX in operation is less than 0.000001 W/m and when key parameters such as the temperature of soil in contact with the heat exchanger and heat flux through the heat exchanger as well as the residual no longer change with iteration.

Model validation has been carried out for a variety of applications of horizontally coupled GHXs buried in loam soil for a period of one to two months [25, 26, 33, 36] and loamy sand soil for six-months [32].

The procedure for simulation of the performance of a GHX is shown in Fig. 12. The simulation involves two stages. The first stage is to generate the vertical soil temperature and moisture profiles for initialisation and the second stage is to predict the GHX performance.

Stage 1: For a given site where the GHX is installed, basic data for the texture of soil and atmospheric (boundary) conditions are obtained. In general, the time-varying boundary conditions are used with varying time steps (Δt) to solve one-dimensional equations (7) and (8) for multi-year HMT processes (or cycles). Results of the vertical profiles of soil temperature and moisture for two consecutive years are then compared. If the temperature difference (ΔT) and moisture difference ($\Delta\Theta$) for any depth and at any time of a year are less than a prescribed small value ε, the profiles corresponding with the time to start operating the GSHP system are taken as the initial values for the depth-varying soil temperature and moisture in the whole computational domain. Vertical profiles for soil properties are also available for initialisation as required for the solution of Equations (7) and (8) but these could alternatively be calculated using Equations (4) to (6) at the beginning of the next stage from the moisture profile. These results, if saved for each month for instance, can be used for simulation of system operation starting from any month of a year. However, if the starting time for the system operation is known beforehand, simulation can start from the moment corresponding to the system's starting time and results need to be compared only for the end of final calculation year instead of whole year, as described before.

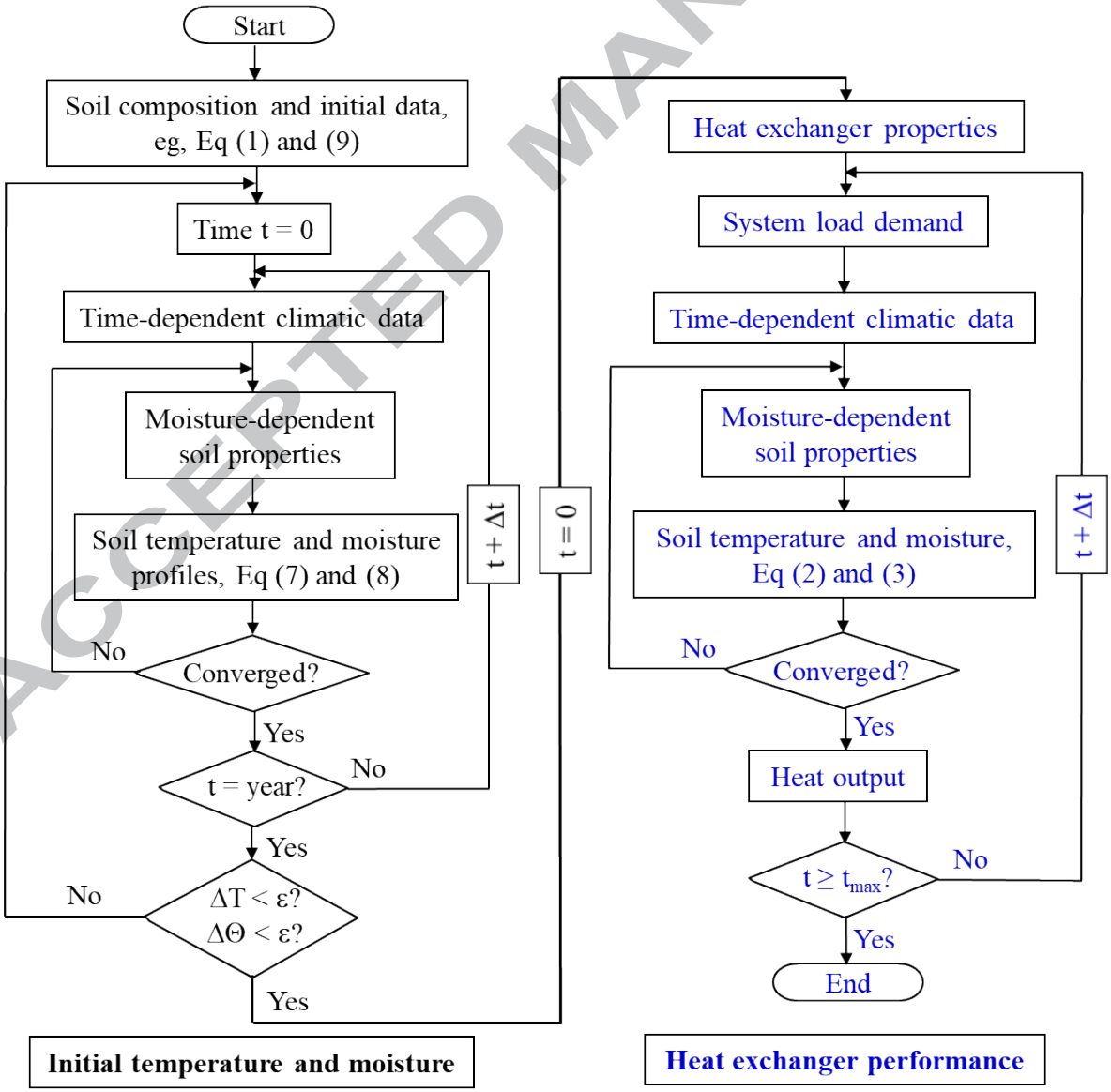

Fig. 12 Procedure for simulation of GHX performance with coupled HMT

Stage 2: The initial temperature and moisture profiles together with time-dependent boundary conditions are used for solving three-dimensional Equations (2) (or 2a) and (3) with the GHX buried in soil for a specified period of system operation (t_{max}). The boundary conditions for the solution include i) the same conditions for the domain boundary as above and ii) the operating conditions for the GHX based on the properties of the heat exchanger and building load demand. If the operating conditions are given as the flow rate and temperature of the fluid, the heat output through the GHX (to meet the building load demand) can be calculated for each time step. Results from the simulation include the history of heat transfer through the GHX and detailed distributions of temperature and moisture in the computational domain as well as spatiotemporally varying soil properties. Finally, if and when required as for the present work, the impact on the GHX performance can be assessed by means of comparison between results from solution of Equations (2) or (2a) and (3) for coupled HMT and from solution of Equation (2a) for heat transfer only with constant soil properties.

3. APPLICATION

The methodology is used to predict the performance of a horizontal straight GHX for heating between October and March with the same climatic conditions as above for the illustration of generating initial moisture and temperature profiles. However, the soil texture is changed to loamy sand. Besides, instead of the bare ground surface and extremely deep water table, it is assumed that the ground surface is half covered with vegetation and that the water table depth is 10 m. The GHX consists of 40 mm HDPE pipes buried between 1 m and 2 m deep. The working fluid for the heat exchanger is a 35/65 mixture of antifreeze and water. The fluid temperature at the inlet is fixed at 1^{o}C. The fluid velocity is 0.5 m/s such that the flow is in the transitional-turbulent region for efficient heat transfer without excessive hydraulic pressure losses [1]. In addition, further predictions are performed for different climatic conditions and for a total of five different types of soil. Table 1 shows the composition and saturation moisture content for five types of soil studied.

Table 1 Composition and saturation moisture of soil

Type of soil	Clay	Clay loam	Loam	Loamy sand	Sand
Composition (proportion of sand, clay and silt) [31]	22 : 58 : 20	32 : 34 : 34	43 : 18: 39	64.4 : 2.4 : 33.2	92 : 3 : 5
Saturation moisture content (m^3/m^3)	0.48	0.45	0.44	0.41	0.37

Simulations are performed using two types of heat transfer model – i) general model involving coupled HMT and this is called the coupled model and ii) model without consideration of moisture transfer and this is called the model with heat transfer only or simply the heat transfer model. The heat transfer model also requires soil properties for simulation and these are calculated using Equations (4) to (6) with a moisture content fixed for the whole season or a constant but non-uniform moisture profile.

Figure 13 shows the predicted vertical temperature and moisture profiles in loamy sand soil at the beginning (midnight) of October and these are used as initial data. The ground surface is quite cool at 6^{o}C, lower than the air temperature of 8.4^{o}C, at the night time as a result of radiation heat transfer from ground surface to the sky. The soil temperature increases with depth rapidly to 13.5^{o}C at 0.3 m deep and then slowly to 15^{o}C at 2.1 m deep from where it decreases gradually with the increase of depth. The soil surface is dry at the time but moisture

increases rapidly with depth at a rate over 0.2 m^3/m^3 per meter to 0.24 m^3/m^3 at 0.2 m deep. The moisture continues to increase at decreasing rates to 0.32 m^3/m^3 at 1.5 m deep but then begins to decrease very slowly to 0.315 m^3/m^3 at about 3 m deep. It is almost uniform between 3 m and 7 m deep and finally increases with depth again to the saturation value.

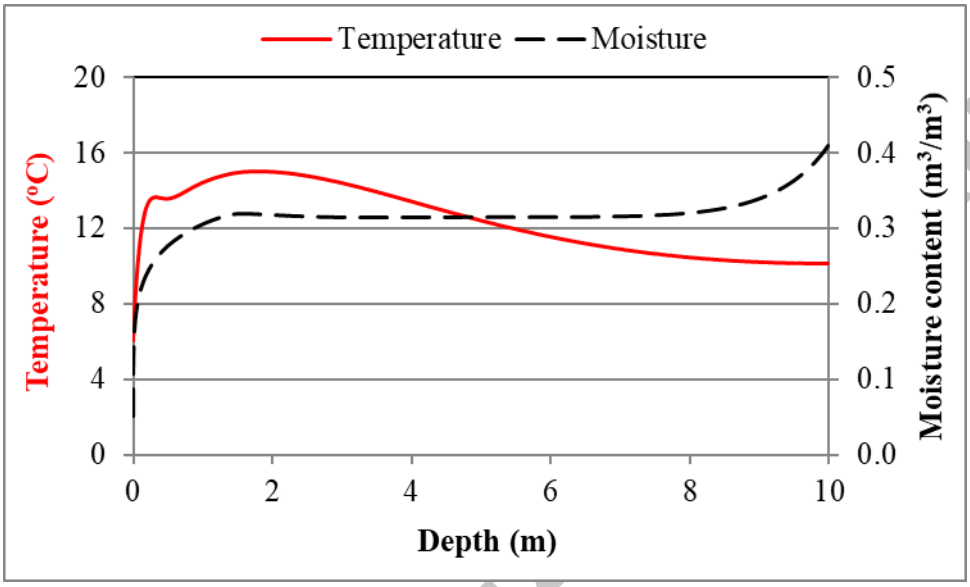

Fig. 13 Predicted initial temperature and moisture variations in loamy sand soil

Figure 14 shows the predicted soil thermal conductivity and diffusivity at the beginning of October. The thermal conductivity is low at 1.07 W/mK for dry soil at the top surface and following the variation pattern of moisture content it increases rapidly to 1.72 W/mK at 0.2 m deep and then gradually to 1.87 – 1.89 W/mK at 1 – 2 m deep, respectively. Both the density and specific heat of soil also increase with depth and as a result the thermal diffusivity decreases with increasing depth from 0.821 x 10^{-6} m^2/s just below the surface to 0.771 – 0.765 x 10^{-6} m^2/s at 1 – 2 m deep, respectively.

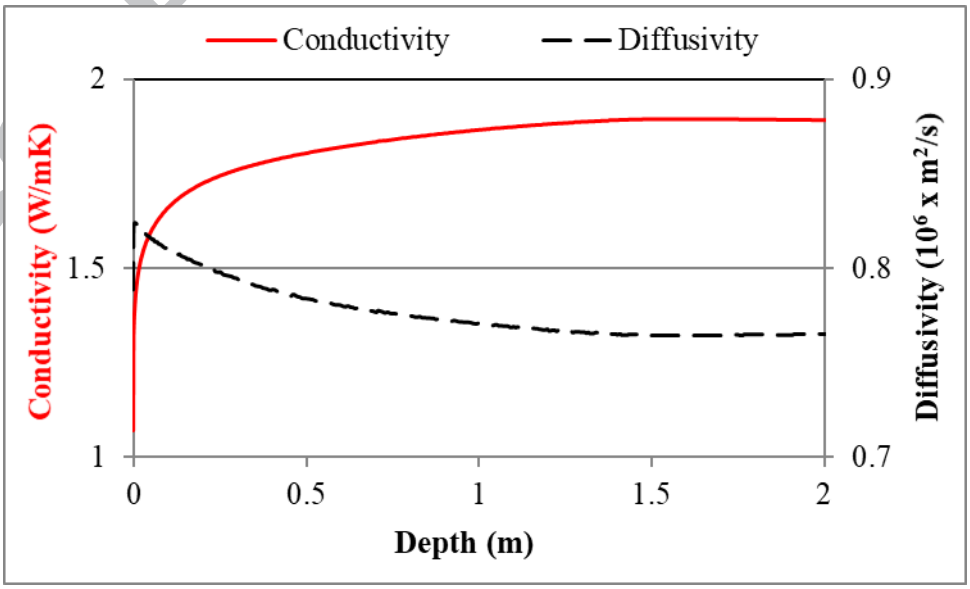

Fig. 14 Predicted variation of initial soil thermal conductivity and diffusivity

To illustrate the spatiotemporal variations in soil moisture and thermal properties, Fig. 15 shows the moisture content and thermal conductivity for the midnight of a day with rain in

the evening before. The soil near the surface is saturated by the time. The moisture decreases with increasing depth up to about 0.6 m. The thermal conductivity also decreases in this layer of soil from 2.07 W/mK at the surface to 1.8 W/mK at 0.6 m deep. Thus, the thermal conductivity could be nearly doubled from dry to wet soil. The corresponding thermal diffusivity increases with depth from 0.726 x 10^{-6} m^2/s at the surface to 0.774 x 10^{-6} m^2/s at 0.6 m deep.

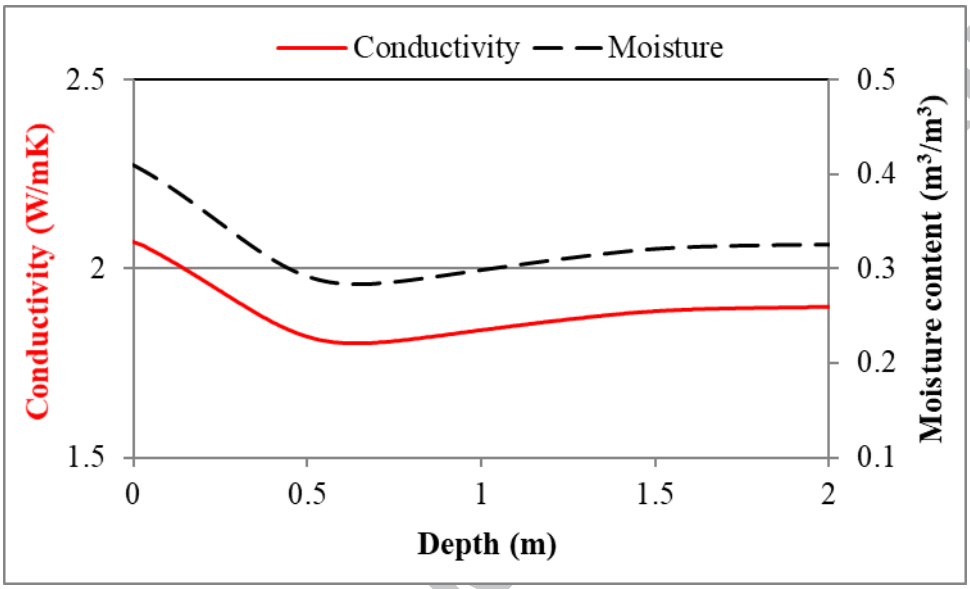

Fig. 15 Predicted variation of soil moisture and thermal conductivity after rain

Figures 16 and 17 show comparisons of the predicted heat transfer rates per unit length of the heat exchanger buried at 1 m and 2 m deep for the heating season using the model with moisture transfer (coupled model) and the model without moisture transfer (heat transfer model) with soil properties at three different moisture levels – uniformly low (0.2 m^3/m^3), uniformly high (0.32 m^3/m^3) and varying with depth.

The overall variation patterns of the predicted heat transfer are similar from both types of model. That is, the heat transfer rate decreases rapidly for the first few hours. The rate of decrease drops afterwards and becomes nearly linear for over two months. Close to the end of the third month (December), the decrease becomes insignificant. The heat transfer rate reaches minimum around the end of January and from then on increases gradually because of rising air temperature which leads to increasing soil temperature.

There are however significant differences in the magnitude of predicted heat transfer between the two types of model and these are illustrated by comparing the coupled model with three examples using the heat transfer model. The first example for the heat transfer model is based on a 0.2 m^3/m^3 moisture content from an on-site measurement [31] for calculating the soil properties. Because this moisture content is lower than that of deeper soil, the heat transfer predicted with the heat transfer model is lower than that with the coupled model. The difference (represented by Difference for mc=20% in Fig. 16(b) and Fig. 17(b) for 1 m and 2 m deep heat exchangers, respectively) varies with installation depth and in general decreases with time for the first three months both in terms of magnitude and percentage. The average difference (under-prediction by the heat transfer model) for the whole season is higher at deeper installation; it is 6.3% for the 1 m deep GHX but is 11.3% for the 2 m deep one. This

is because the moisture-dependent soil properties at a greater depth are much higher than the calculated values with the assumed low moisture content.

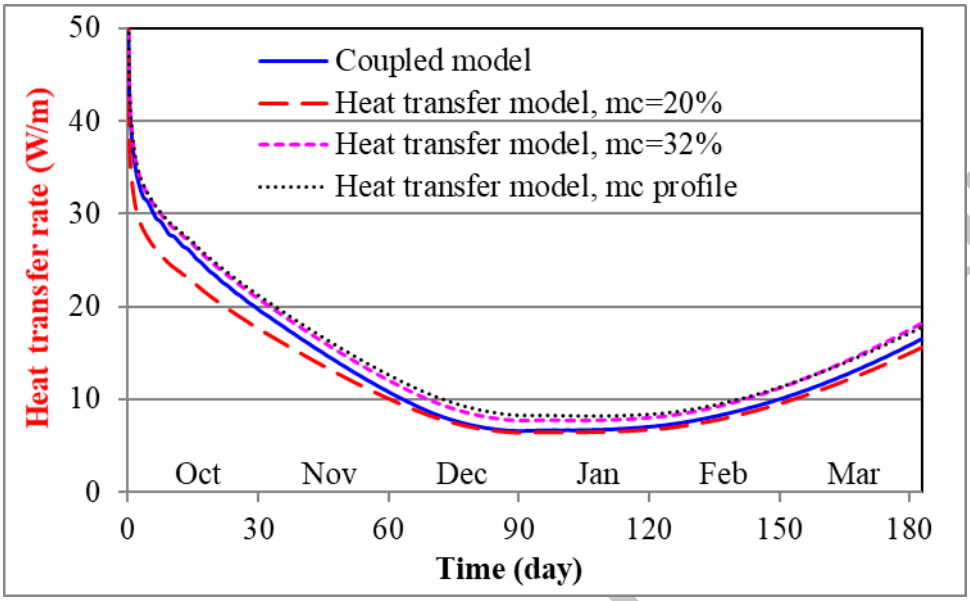

(a) Predicted heat transfer rate

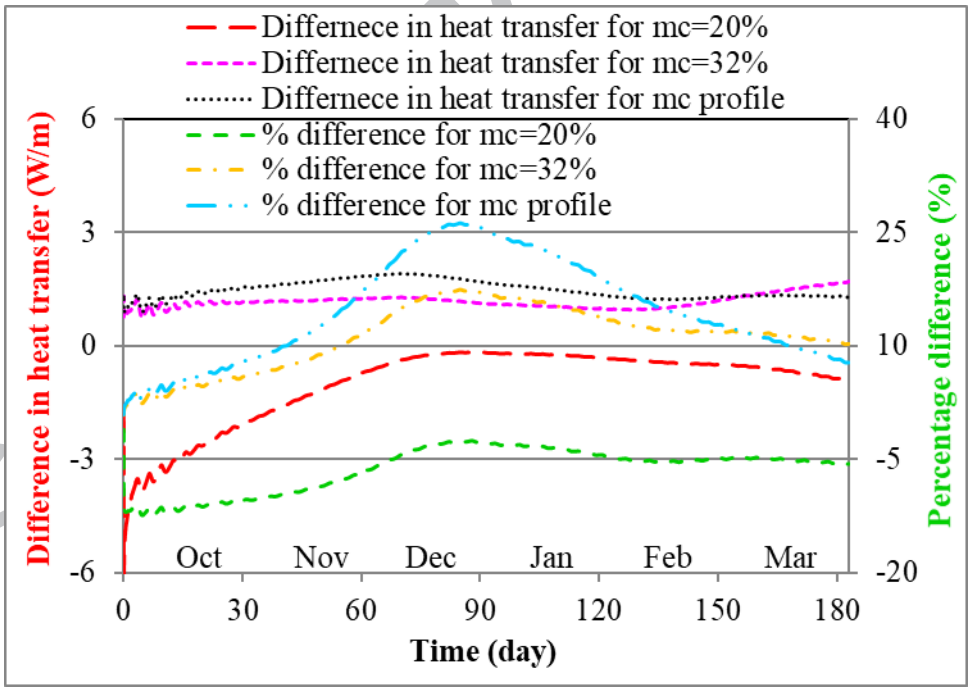

(b) Difference from the coupled model

Fig. 16 Comparison between two models for predicting the heat transfer rate through the 1 m deep GHX

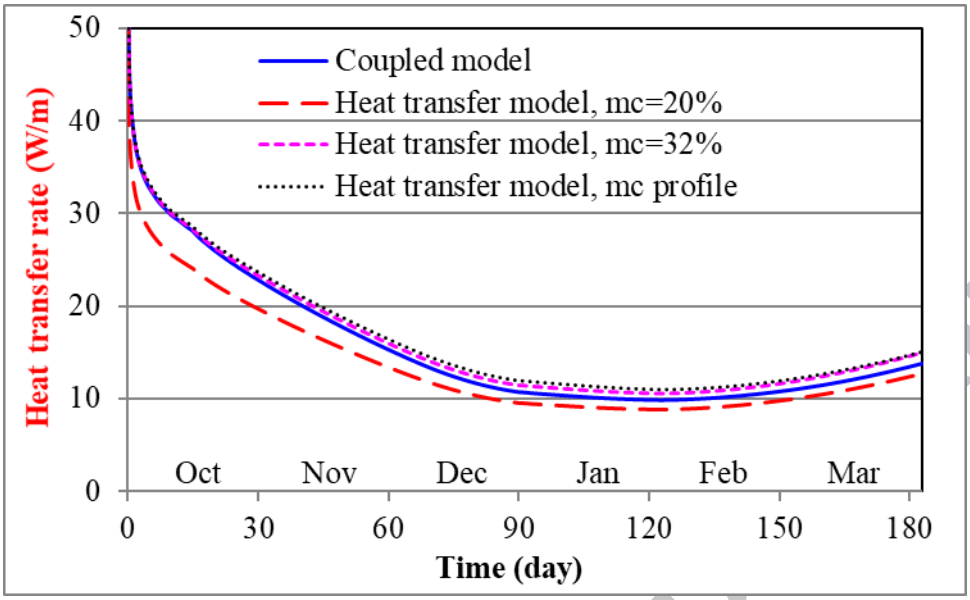

(a) Predicted heat transfer rate

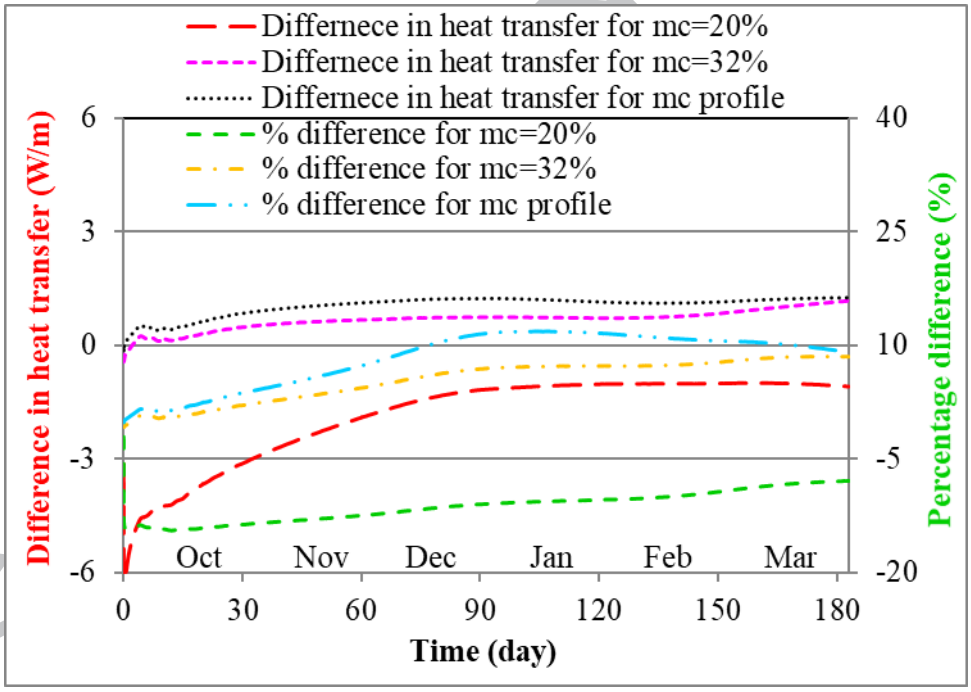

(b) Difference from the coupled model

Fig. 17 Comparison between two models for predicting the heat transfer rate through the 2 m deep GHX

The changing difference in the output for heat transfer between the two models implies that a heat transfer model without consideration of moisture transfer is not capable of accurately predicting the dynamic performance of a horizontal GHX even if use could be made of accurate soil properties eg measured at the installation depth. This is compared in Fig. 16 and Fig. 17 as the second example for the heat transfer model with a 0.32 m^3/m^3 (ie, mc=32%) moisture content – the mean value for the whole heating season at the installation depths - for the calculation of soil properties. The two models would produce the same heat transfer rate only at the beginning. Using the heat transfer model would however result in over-prediction

of heat transfer and the difference again varies with depth and time. For the 1 m deep GHX, the level of over-prediction is fairly constant at about 1 W/m. However, in terms of percentage change in relation to the prediction from the coupled model, it increases with operating time by up to 17.4% at the end of December and then decreases slightly with increasing time. For the 2 m deep GHX, the level would increase with time continuously both in magnitude and percentage. The seasonal average level of over-prediction is 11.2% for the 1 m deep GHX, twice as large as that for the 2 m deep one, i.e. 5.5%.

In the third example, the initial moisture profile in Fig. 13 is used to calculate spatially varying but temporally constant soil properties for the heat transfer model. It is seen from Fig. 16 and Fig. 17 for the lines with mc profile that the heat transfer model would over predict heat transfer. The level of over-prediction would increase with time slightly in magnitude but significantly in percentage terms for the first three months or so. It increases to a maximum of 26.2% in December for the 1 m deep GHX and 11.8% in January for the 2 m deep one and then decreases afterwards. The average differences for the heating season are 14.4% and 8.3%, respectively, for the 1 m and 2 m GHXs. These are even larger than those predicted using a uniform moisture content representative at the installation depths for the calculation of soil properties. The reason for such worse results is that the poor thermal conductivity of dry soil near the ground surface reduces the heat loss from soil to cold ambient air in the early part of the heating season. Therefore, the accuracy of predicting dynamic thermal performance using a heat transfer model could not be improved unless consideration is given to both spatially and temporally varying soil properties.

3.1 Effect of the external environment

The external environment consists of a set of atmospheric conditions that interact with soil at the ground surface. Here only two key parameters that are directly associated with moisture in air and soil - rainfall (precipitation) and the partial water vapour pressure of atmosphere - are selected to assess the impact of the external environment on the soil properties and resulting performance of the GHX. The level of rainfall and the vapour pressure are halved separately and in combination to simulate the drier climatic conditions. For each set of the atmospheric conditions, the initial temperature and moisture profiles are first generated using the same method as described previously. Fig. 18 shows the initial moisture profiles for the three scenarios as well as the case with the original (normal) conditions denoted as the base case. Reducing rainfall or vapour pressure results in lower soil moisture and thermal properties but the influence of rainfall is less than that of vapour pressure. In particular, the influence of reducing rainfall on soil moisture up to 1 m deep is negligible at this time. The overall vertical moisture profile for the reduced rainfall may be explained as follows: in summer reduced rainfall leads to lower downward flow of moisture but in autumn this amount of rainfall would be sufficient to recharge shallow soil at the site. Another explanation for this apparent insignificance of rainfall reduction is the associated assumption for the top boundary – excess rainwater to run off during rain [25]. Thus, if the reduced rainfall would still be able to saturate the top soil during the same period of rain, the intensity of rain above such a level would have little effect on soil moisture absorption theoretically.

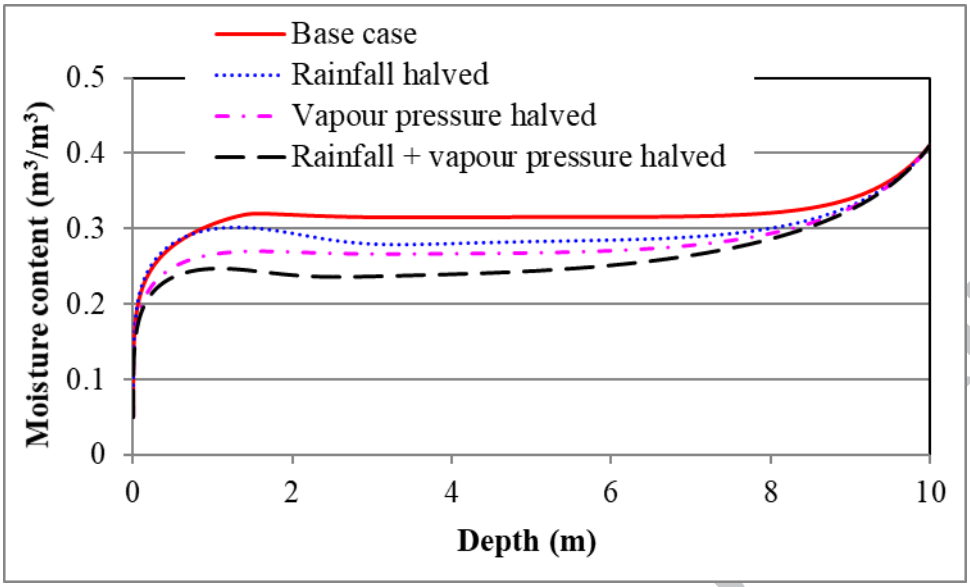

Fig. 18 Effect of atmospheric conditions on the predicted initial soil moisture content

Comparison of the predicted performance is carried out for the 1.5 m deep GHX. The predicted initial soil moisture content at 1.5 m depth is 32%, 30.1%, 26.8% and 24.7%, respectively, for the base case and the cases with reduced rainfall, vapour pressure and both reduced rainfall and vapour pressure. Fig. 19 shows that the overall trend of variation of heat transfer with time is again similar for different external environmental conditions. The heat transfer rate decreases as a result of the reduction in the rainfall or vapour pressure or both. The decrease due to the reduced rainfall is relatively stable for the first half of the heating season but becomes less with time for the second half of the season. In contrast, the decrease due to the reduced vapour pressure or in combination with rainfall rises gradually with time for the first half of the season but drops rapidly for the second half. The average decreases in heat transfer for the first half of the season are about 7%, 12% and 13% due to the reduced rainfall, vapour pressure and a combination of both, respectively. It is thus confirmed from Fig. 19 that decreasing the vapour pressure has a larger influence on the heat transfer than decreasing rainfall. Basically, if rainfall is reduced while the vapour pressure remains the same, the moisture evaporation rate from soil to air would not increase much in dry times. However, if the vapour pressure is reduced while the amount of rainfall keeps unchanged, the increase in the surface moisture evaporation would be more than the replenishment of soil moisture by rain. Consequently, the soil becomes drier, leading to its lower thermal properties and poorer GHX performance.

Another finding from the simulations is that the effects of reduced rainfall and vapour pressure are not simply additive - the overall effect is less than the sum of two. The mean decrease in heat transfer for the heating season due to the combined reduction of rainfall and vapour pressure is about 12% compared with 5% and 11% respectively for the reductions in rainfall and vapour pressure separately.

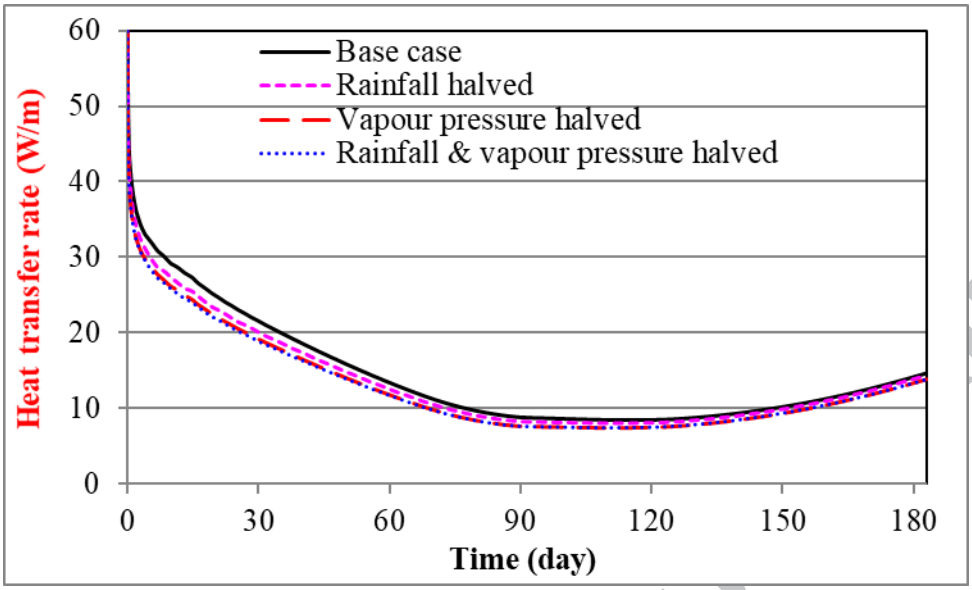

(a) Predicted heat transfer rate

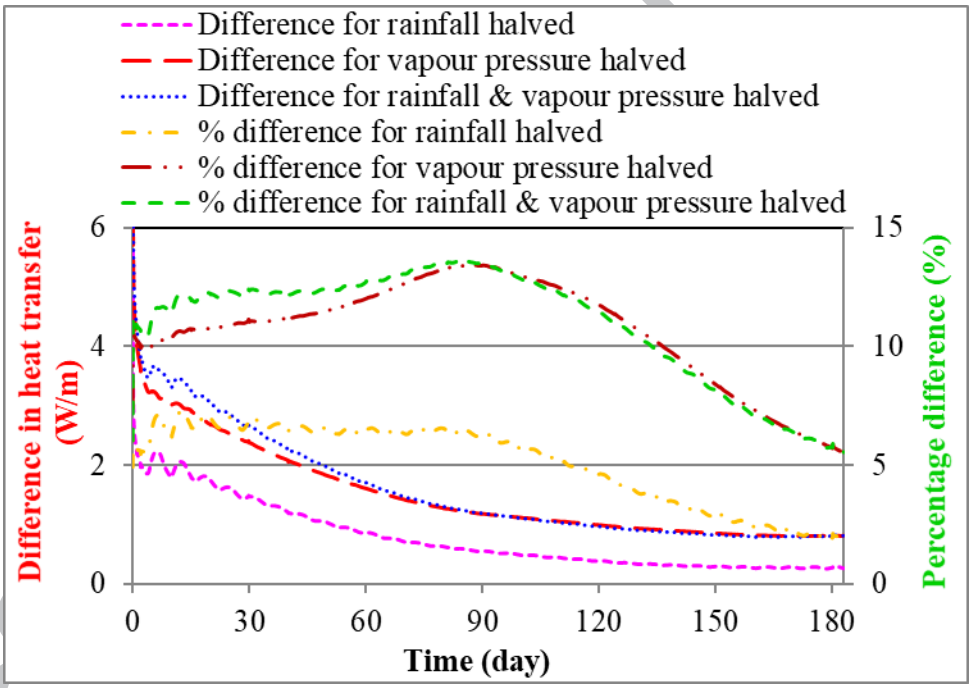

(b) Difference from the base case

Fig. 19 Effect of the external environment on the heat transfer through the GHX

Again, the impact of coupled HMT depends on the initial soil moisture. For soil properties calculated with a 0.2 m^3/m^3 moisture content, heat transfer would be under predicted using the model without coupled moisture transfer. The level of under-prediction would generally decrease with increasing operating time for the whole season with the reduced rainfall, but only for the first half of the season with the reduced vapour pressure or in combination with rainfall, as shown in Fig. 20a. Besides, the reduction of rainfall would have the highest impact. Estimating the soil properties with a 0.32 m^3/m^3 moisture content would reverse the relative influence for these parameters (Fig. 20b compared with Fig, 20a). The heat transfer rate would be over predicted with the model without moisture transfer and the impact of rainfall reduction becomes less than that of vapour pressure. This is because moisture at the

installation depth due to the reduced rainfall (30.1% or 0.301 m^3/m^3) is closer to the value with the original conditions (0.32 m^3/m^3) than those involving reduction in the vapour pressure (0.247 to 0.268 m^3/m^3). Hence, when the calculation of soil properties is based on the predicted moisture profile with the individual set of atmospheric conditions but set the value at the installation depth for the whole domain, the difference between the reduced rainfall and vapour pressure becomes much less and their impact is generally less than that for the original conditions as shown in Fig. 20c. Besides, the heat transfer model would under predict heat transfer for the first month or so but over predict it for most of the heating season with a maximum difference of about 9% for the case with reduced rainfall. The level of over-prediction averaged over the heating season is 4%, 6% and 4% for reduced rainfall, vapour pressure and both together, respectively.

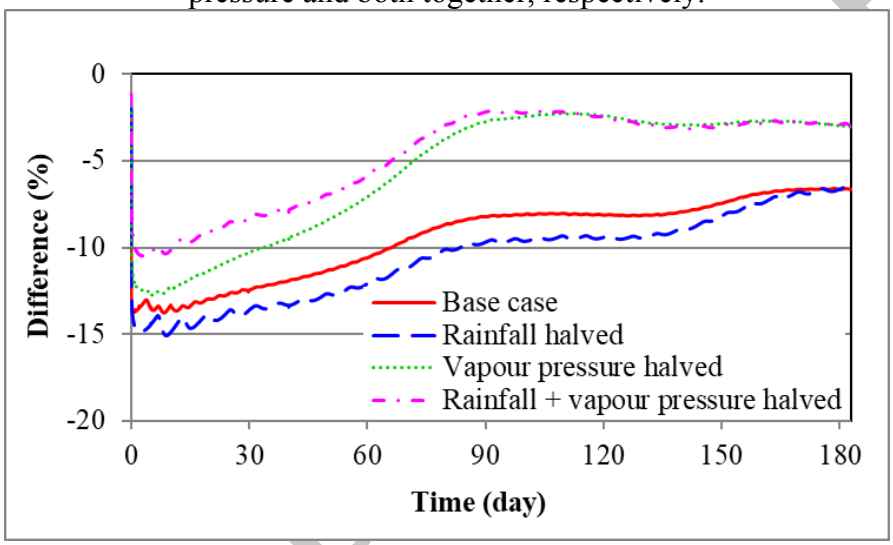

(a) With a uniform moisture content of 0.2 m^3/m^3

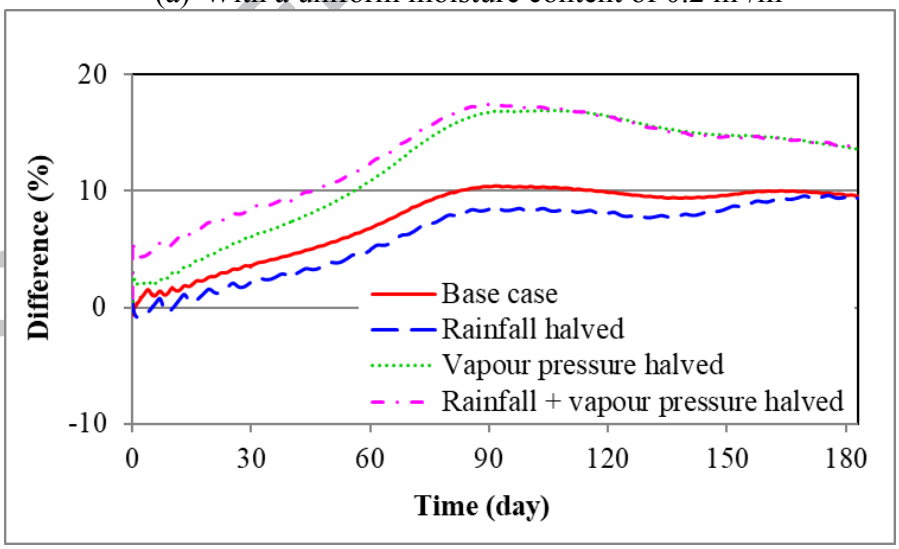

(b) With a uniform moisture content of 0.32 m^3/m^3

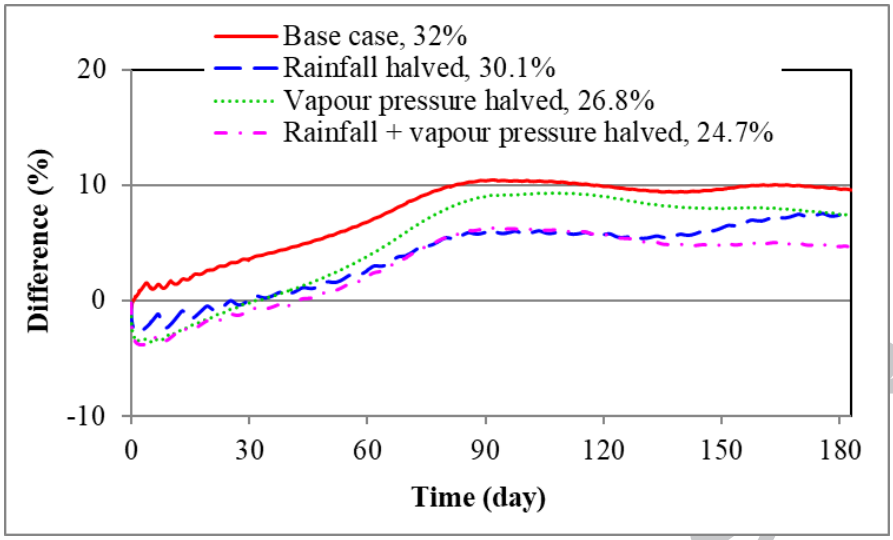

(c) With a uniform moisture content for each set of conditions

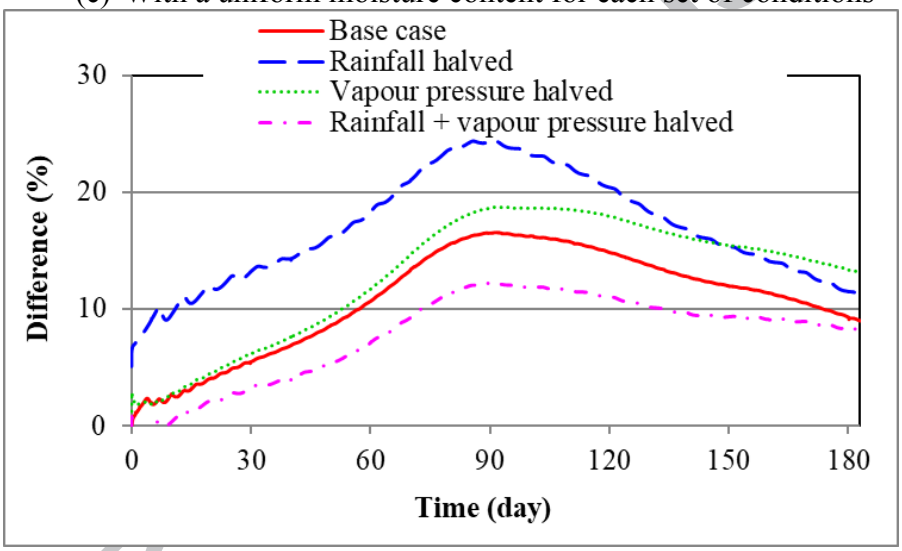

(d) With initial moisture profiles

Fig. 20 Effect of the external environment on the difference in heat transfer between the coupled model and the heat transfer model (positive for over-prediction and negative for under-prediction)

When the soil properties are spatially varying but temporally constant based on the initial moisture profile, the heat transfer rate would be over predicted and the level of over-prediction would increase with increasing time up to 24%, 19% and 12% in December when the rainfall, vapour pressure and their combination are halved, respectively, compared with 17% for the base case, and then decreases almost linearly to 11%, 13% and 8% respectively at the end of the season (Fig. 20d). The effect of reduced rainfall is generally larger than that of reduced vapour pressure which is larger than the effect from combined reduction of vapour pressure and rainfall, with average over-prediction of 17%, 13% and 8% for the whole season, respectively. The impact of reduced rainfall and vapour pressure is summarised symbolically in Table 2.

Table 2 Impact of rainfall and vapour pressure on the thermal performance of a horizontal GHX predicted with the heat transfer model at selected soil moisture levels

Moisture for calculation of soil properties	Reduced rainfall	Reduced vapour pressure	Reduced rainfall and vapour pressure
0.2 m^3/m^3	⇓	↓	↓
0.32 m^3/m^3	↑	⇑	⇑
Value at installation depth	↑	↑	↑
Moisture profile	⇑	⇑	↑

↑ - over-prediction
↓ - under-prediction
⇑ - over-prediction and more than the value predicted under normal atmospheric conditions
⇓ - under-prediction and more than the value (magnitude) predicted under normal atmospheric conditions

3.2 Effects of installation depth and soil texture

To investigate the effects of installation depth and soil texture on the predicted performance of a GHX, further simulations are performed using the coupled model for the GHX at five depths (1, 1.2, 1.5, 1.8 and 2 m) in four more types of soil – clay, clay loam, loam and sand in addition to loamy sand, see Table 1 for their composition of solid matters.

Figure 21 shows the vertical variations in the moisture content and thermal diffusivity at the beginning of October for the five types of soil. The moisture content in the clay soil is highest while that in sandy soil is lowest. By contrast, sandy soil has the highest thermal diffusivity and clay soil has the lowest, largely because of the proportion of sand in the five types of moist soil. Also, the variation with depth is much less for the diffusivity in clay or clay loam soil. The properties for loam soil lie between those for clay loam and loamy sand soils but are closer to the former. Consequently, the capacity of a GHX to extract heat from soil would be in the same order as that of the soil properties.

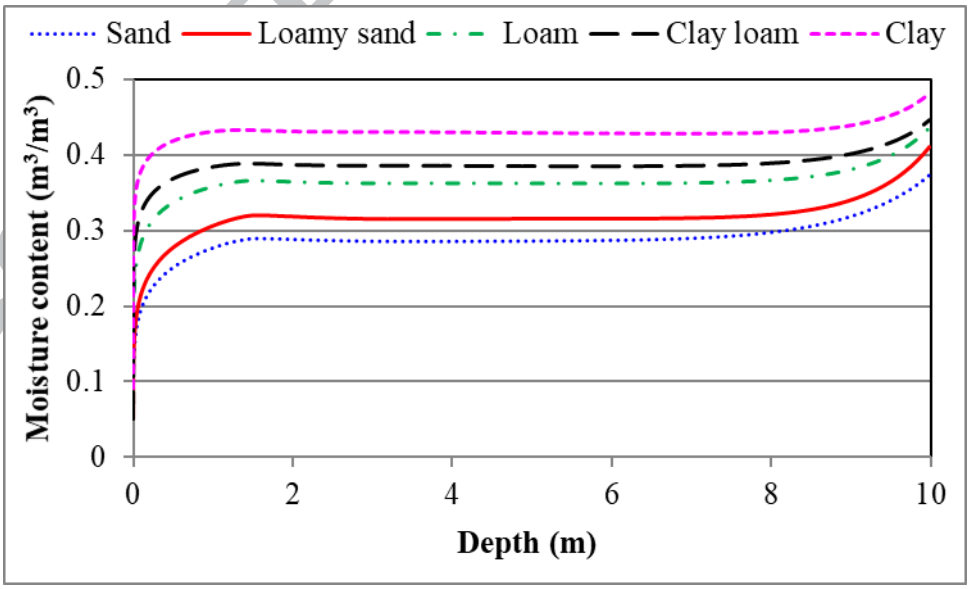

(a) Moisture content

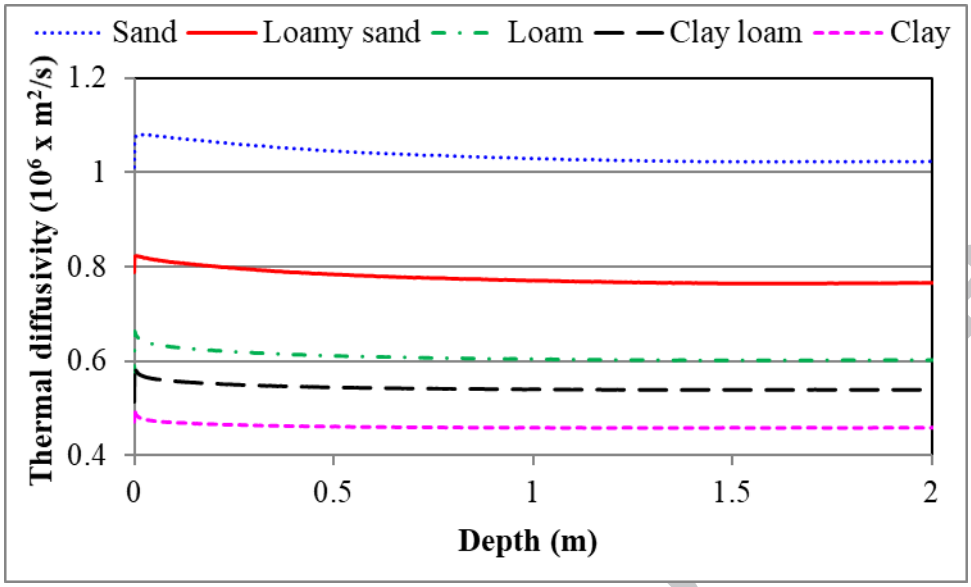

(b) Thermal diffusivity

Fig. 21 Initial moisture content and thermal diffusivity for five types of soil

The temporal variation patterns of heat transfer are similar for different depths and soil types. Fig. 22 shows the monthly total heat extraction per unit length of the heat exchanger for three installation depths while Fig. 23 shows the seasonal total heat extraction for five depths in five types of soil. In general, the monthly heat extraction increases with installation depth of the heat exchanger because the soil moisture and temperature increase with depth in most months of the heating season. The effect of the depth varies with operating time with the largest difference in the heat extraction in December. The difference decreases gradually in the new calendar year so much so that the heat extraction through the heat exchanger in a shallower ground becomes higher in March due to gradual warming of soil from top by atmosphere, which is further explored later.

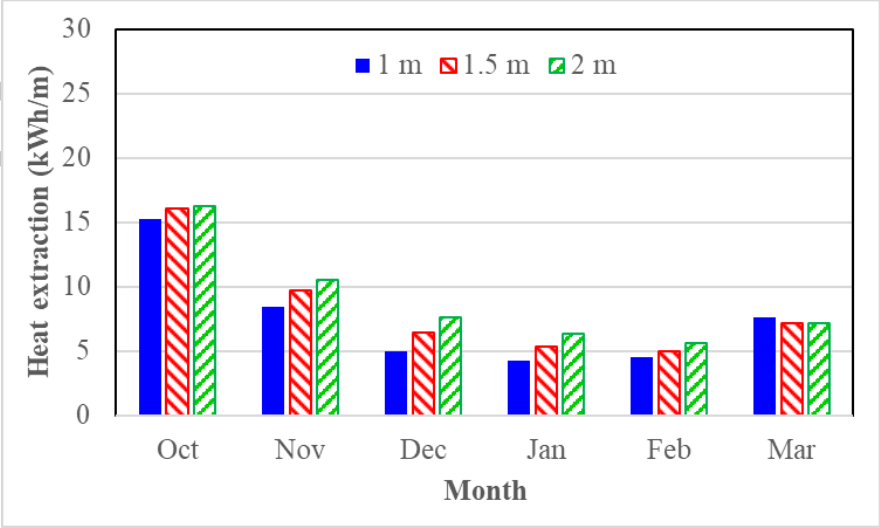

(a) Clay soil

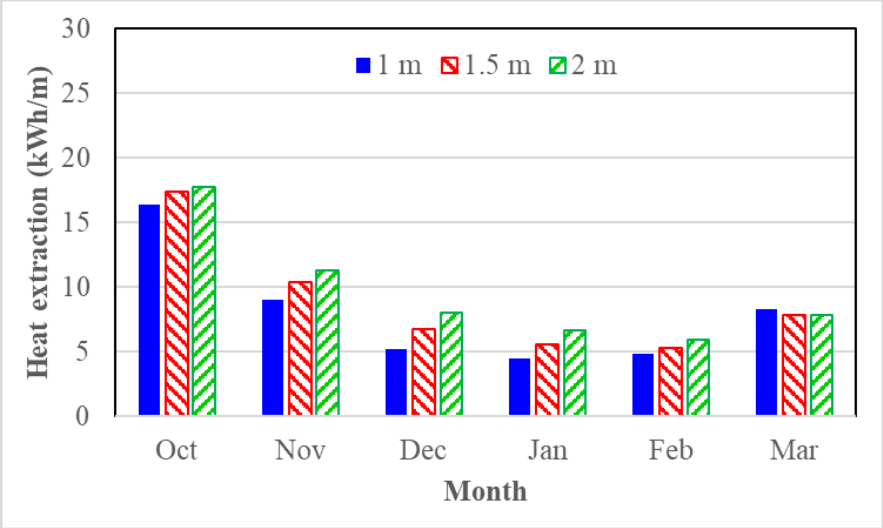

(b) Clay loam soil

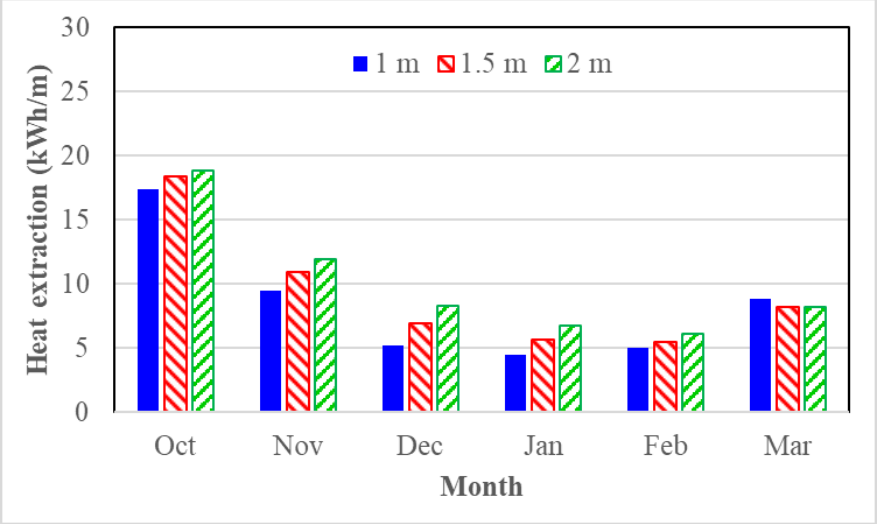

(c) Loam soil

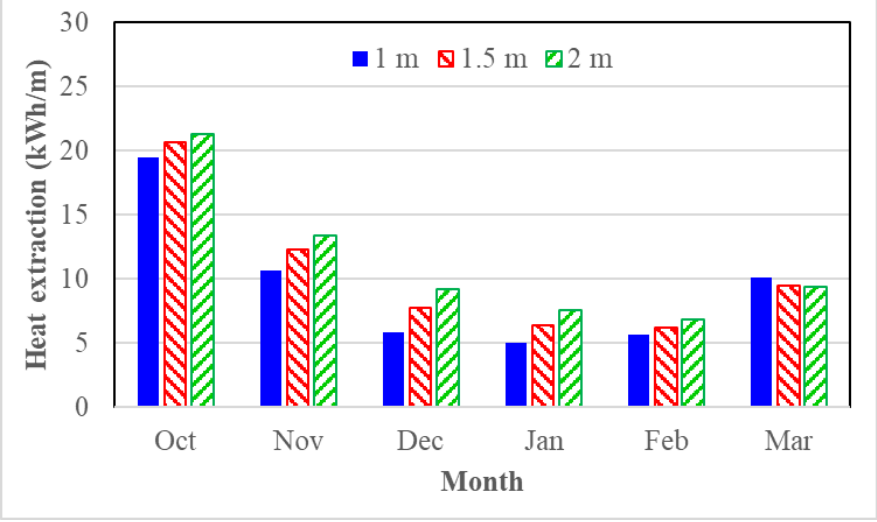

(d) Loamy sand soil

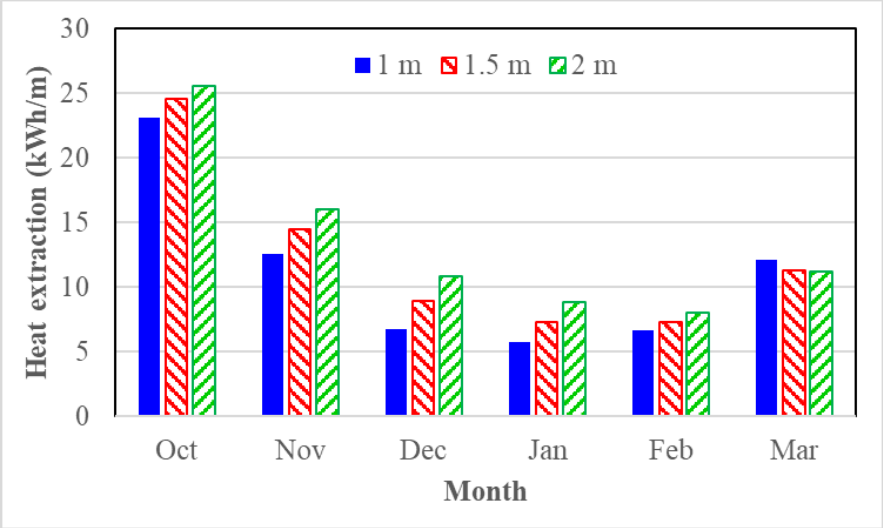

(e) Sandy soil

Fig. 22 Predicted monthly heat extraction at three installation depths in five soil types

The total heat extraction for the heating season (183 days or 4392 hours) from clay soil increases from 44.8 kWh/m for the GHX installed at 1 m deep to 53.4 kWh/m at 2 m deep. The total heat extraction from clay loam soil (48.2 to 57.5 kWh/m), loam soil (50.3 to 60.3 kWh/m), loamy sand soil (56.8 to 67.7 kWh/m) and sandy soil (66.9 to 80.4 kWh/m) is on average 8%, 13%, 27% and 50%, respectively, higher than that in clay soil. Besides, the difference in seasonal heat extraction is almost independent of the installation depth with a maximum difference of 1% for all but sandy soil which varies by a maximum of 1.5% as shown in Fig. 23.

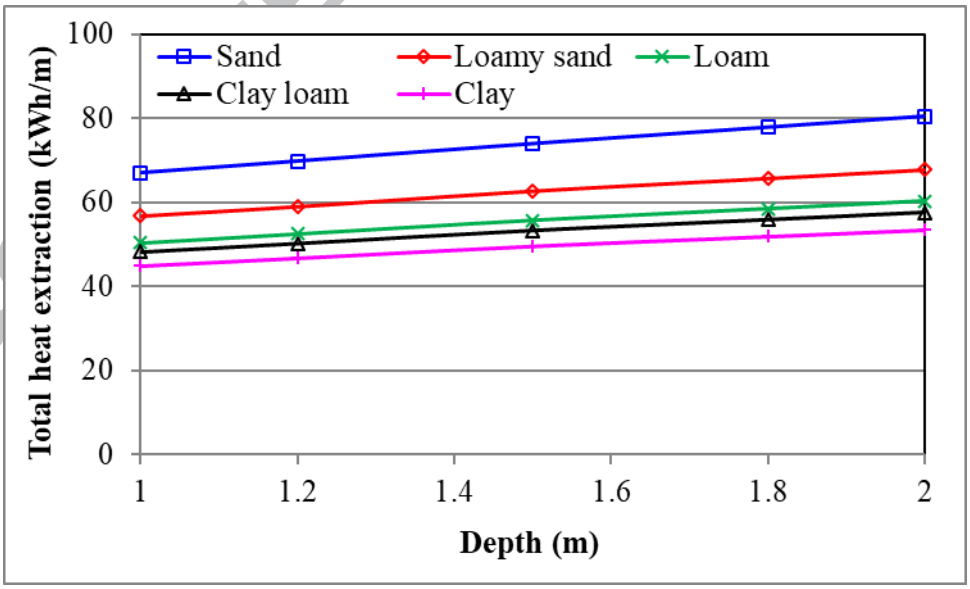

(a) Total heat extraction

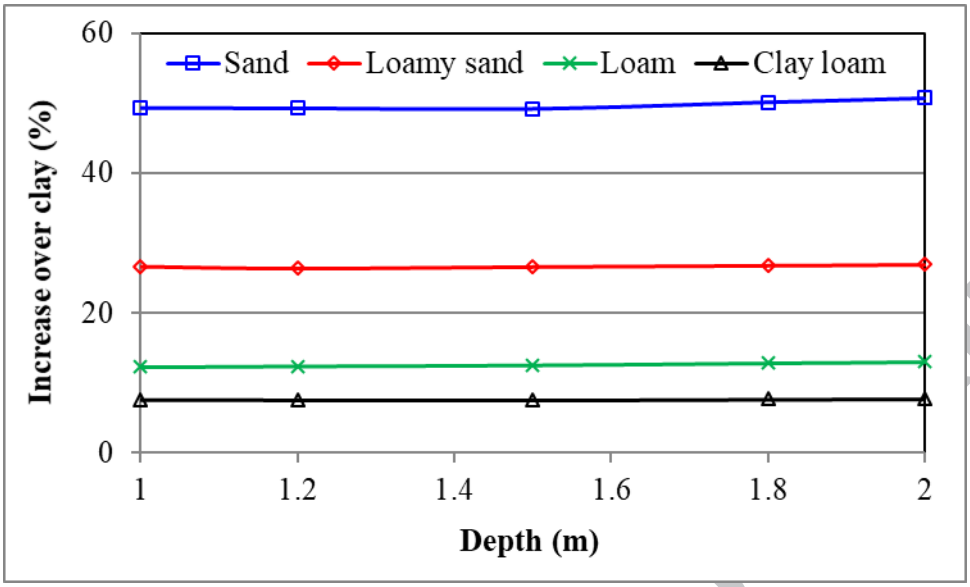

(b) Increase over clay soil

Fig. 23 Predicted total heat extraction at different installation depths in different soil types

The variation of heat extraction with time and installation depth can be explained from the corresponding variation in soil temperature in combination with heat transfer through the heat exchanger. Fig. 24(a) shows five vertical temperature profiles without a heat exchanger (denoted as profile) at the beginning of October, November, December, January and March and four predicted temperature variation patterns along a vertical line through a heat exchanger installed in loamy sand soil at 1.5 m deep (denoted as predicted) at the beginning of November, December, January and March. Fig. 24(b) and Fig. 24(c) show the predicted temperature variations with the heat exchanger installed at three different depths at the beginning of January and the end of March, respectively, together with the corresponding vertical temperature profiles without the heat exchanger. The natural soil temperature (profile) decreases with time up to 6 m deep until early January due to decreasing air temperature. The decrease in the predicted soil temperature is accelerated by heat extraction (relative to the temperature profile). The extent of temperature decrease increases with the depth of heat exchanger but the soil temperature surrounding the heat exchanger is still higher with deeper installation of the heat exchanger in January (Fig. 24 (b)). Hence, the heat extraction rate is larger for the deeper heat exchanger by the time. However, because of the larger heat extraction, the soil temperature decreases faster and consequently the relative difference in the heat extraction rate between deeper and shallower heat exchangers decreases from then on and at some point in spring the soil temperature and heat transfer rate become higher for a shallower heat exchanger as the top soil warms up in spring and this is shown in Fig. 24(c) for soil temperatures at the end of March.

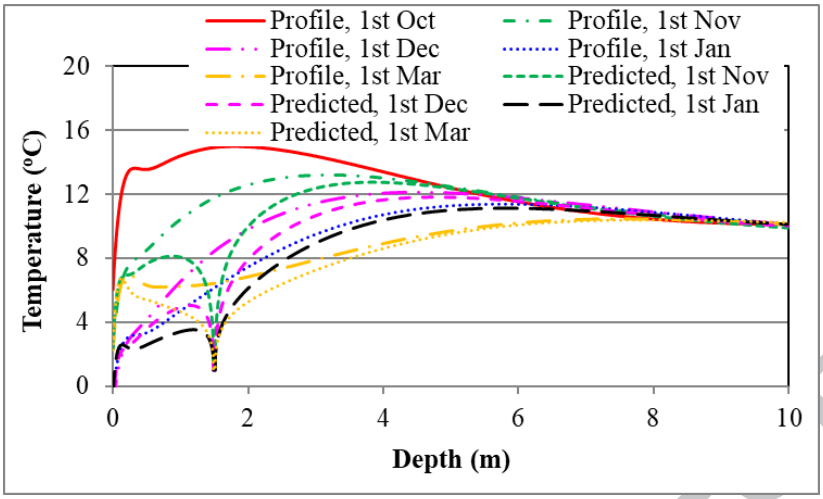

(a) Temperature profile and predicted temperature at different times with GHX at 1.5 m deep

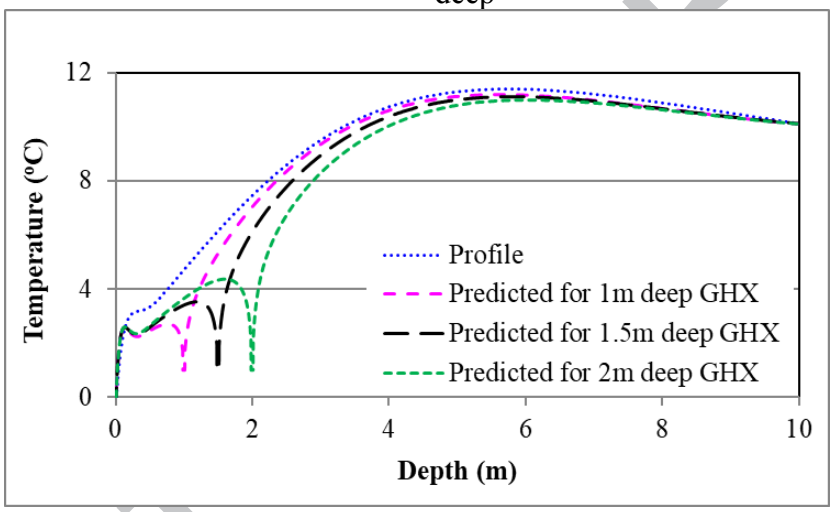

(b) Soil temperature with GHX at three depths at the beginning of January

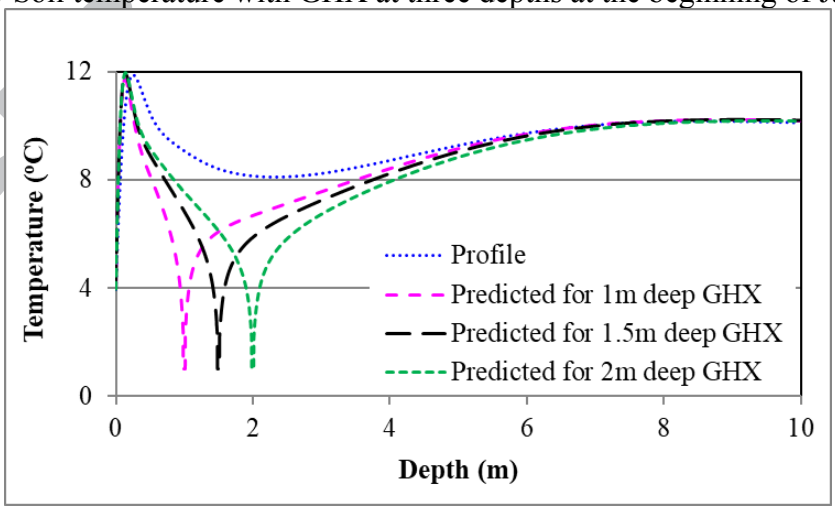

(c) Soil temperature with GHX at three depths at the end of March

Fig. 24 Predicted soil temperatures at different installation depths and operating times

4. CONCLUSIONS

A methodology that accounts for spatiotemporal variations in soil temperature, moisture and thermophysical properties has been presented for comprehensive assessment of the dynamic thermal performance of horizontal GHXs. Spatially varying soil temperature and moisture are generated for any time of a year using one-dimensional coupled HMT equations and used as initial conditions for simulation of three-dimensional transient HMT.

The performance of a GHX is influenced by the soil texture and installation depth as well as the atmospheric conditions. The average heat transfer through a GHX is 8%, 13%, 27% and 50% higher in clay loam soil, loamy soil, loamy sand soil and sandy soil, respectively, than in clay soil, in a climate of England. The seasonal total heat extraction increases with the installation depth of a GHX although daily or monthly heat extraction could be higher in a shallower ground in March and later when the soil temperature rises. The rate of heat transfer is lower when air and/or soil are drier. The seasonal heat transfer would decrease by 5%, 11% and 12% when the rainfall, vapour pressure and both of them are halved, respectively.

The soil properties depend on the moisture content. A heat transfer model without coupling with moisture transfer would not be capable of accurate prediction of the dynamic performance of a horizontal GHX and errors arising from such a model vary with the operating time, GHX depth, soil type and atmospheric conditions. The larger the difference between the soil moisture used for estimating the constant soil properties in the heat transfer model and the spatiotemporally varying soil moisture and properties, the larger the error for a GHX buried at a depth and/or in a type of soil. The impact of atmospheric conditions in terms of vapour pressure and rainfall is more complicated. A heat transfer model would under or over predict the heat transfer rate, respectively, when too low (eg 0.2 m^3/m^3) or too high (0.32 m^3/m^3) a moisture content is used for the calculation of soil properties. The level of under-prediction decreases when the vapour pressure is reduced but increases when rainfall is reduced. In contrast, over-prediction increases with reduced vapour pressure but decreases with reduced rainfall. If the soil properties are calculated with the moisture content representative at an installation depth, the level of over-prediction decreases with the reduction of either rainfall or vapour pressure. However, if a spatially varying but temporally constant moisture profile for soil with a dry surface is used for the calculation, over-prediction increases when the rainfall or vapour pressure is increased but decreases when both rainfall and vapour pressure are reduced.

The methodology can be used not only for systems with a horizontal GHX including horizontal-coupled GSHP and earth air ventilation systems but also for those with a vertical GHX installed in shallow ground where varying atmospheric conditions have significant impacts on the system performance such as energy piles or foundation heat exchangers and borehole GSHPs without adequate thermal and moisture control near the ground surface.

REFERENCES

1. D. Banks, An introduction to thermogeology: Ground source heating and cooling (2nd Edition), John Wiley & Sons, Chichester, 2012.
2. J.D. Spitler, S. Javed and R.K. Ramstad, Natural convection in groundwater-filled boreholes used as ground heat exchangers, Applied Energy, 164 (2016) 352-365.
3. J. Xi, Y. Li, M. Liu, R.Z. Wang, Study on the thermal effect of the ground heat exchanger of GSHP in the eastern China area, Energy, 141 (2017) 56-65.
4. P. Eskilson, Thermal analysis of heat extraction boreholes. PhD Thesis, University of Lund, Sweden (1987).

5. E. Kim, M. Bernier, O. Cauret, J.J. Roux, A hybrid reduced model for borehole heat exchangers over different time-scales and regions, Energy, 77 (2014) 318-326.
6. E. Zanchini, S. Lazzari, New *g-functions* for the hourly simulation of double U-tube borehole heat exchanger fields, Energy, 70 (2014) 444-455.
7. H. Demir, A. Koyun, G. Temir, Heat transfer of horizontal parallel pipe ground heat exchanger and experimental verification, Applied Thermal Engineering, 29 **(**2009) 224–233.
8. H. Esen, M. Inalli, M. Esen, Numerical and experimental analysis of a horizontal ground-coupled heat pump system, Building and Environment, 42 (2007) 1126–1134.
9. Y. Wu, G. Gan, A. Verhoef, P.L. Vidale, R.G. Gonzalez, Experimental measurement and numerical simulation of horizontal-coupled slinky ground source heat exchangers, Applied Thermal Engineering, 30 (2010) 2574-2583.
10. H. Fujii, K. Nishi, Y. Komaniwa, N. Chou, Numerical modeling of slinky-coil horizontal ground heat exchangers, Geothermics, 41 (2012) 55-62.
11. M. Esen, T. Yuksel, Experimental evaluation of using various renewable energy sources for heating a greenhouse, Energy and Buildings, 65 (2013) 340–351.
12. D. Adamovskya, P. Neubergerb, R. Adamovsky, Changes in energy and temperature in the ground mass with horizontal heat exchangers - The energy source for heat pumps, Energy and Buildings, 92 (2015) 107–115.
13. A. B. Platts, D. A. Cameron, J. A. Ward, Validation of a model for two horizontal ground coupled heat exchangers based on field testing, Energy and Buildings, 138 (2017) 11–25.
14. H. Li, K. Nagano, Y. Lai, A new model and solutions for a spiral heat exchanger and its experimental validation, International Journal of Heat and Mass Transfer, 55 (2012) 4404–4414.
15. S. Naylor, S.M. Kevin, M. Ellett, A.R. Gustin, Spatiotemporal variability of ground thermal properties in glacial sediments and implications for horizontal ground heat exchanger design, Renewable Energy, 81 (2015) 21-30.
16. G. Gan, J.L. Woods, A deep bed simulation of vegetable cooling, Proceedings of the 11th International Congress on Agricultural Engineering, Dublin, Ireland, 4 (1989) 2301-2308.
17. J. Wang, N. Christakis, M.K. Patel, M.C. Leaper, M. Cross, A computational model of coupled heat and moisture transfer with phase change in granular sugar during varying environmental conditions, Numerical Heat Transfer – Part A, 45 (2004) 751–776.
18. G. Gan, Effect of combined heat and moisture transfer on the predicted indoor thermal environment, Indoor + Built Environment, 5 (1996) 170-180.
19. D.Q. Yang, H. Rahardjo, E.C. Leong, V. Choa, Coupled model for heat, moisture, air flow and deformation problems in unsaturated soil, Journal of Engineering Mechanics, 124 (1998) 1331-1338.
20. M. Bittelli, F. Ventura, G.S. Campbell, R.L. Snyder, F. Gallegati, P.R. Pisa, Coupling of heat, water vapor, and liquid water fluxes to compute evaporation in bare soils, Journal of Hydrology, 362 (2008) 191– 205.
21. P. Rajeev, D. Chan, J. Kodikara, Ground–atmosphere interaction modelling for long-term prediction of soil moisture and temperature, Canadian Geotechnical Journal, 49 (2012) 1059-1073.
22. H. Xu. and J. D. Spitler, The relative importance of moisture transfer, soil freezing and snow cover on ground temperature prediction, Renewable Energy, 72 (2014) 1-11.
23. M. Chalhoub, M. Bernier, Y. Coquet, M. Philippe, A simple heat and moisture transfer model to predict ground temperature for shallow ground heat exchangers, Renewable Energy, 103 (2017) 295-307.

24. V.R. Tarnawski, P.K Yuet. Winter performance of residential heat pump, Heat Recovery Systems and CHP, 8 (1988) 271-278.
25. G. Gan, Dynamic interactions between the ground heat exchanger and environments in earth–air tunnel ventilation of buildings, Energy and Buildings, 85 (2014) 12–22.
26. G. Gan, Dynamic thermal simulation of horizontal ground heat exchangers for renewable heating and ventilation of buildings, Renewable Energy, 103 (2017) 361-371.
27. O. Ozgener, L. Ozgener, J.W. Tester, A practical approach to predict soil temperature variations for geothermal (ground) heat exchangers applications, International Journal of Heat and Mass Transfer, 62 (2013) 473–480.
28. F. Droulia, S. Lykoudis, I. Tsiros, N. Alvertos, E. Akylas, I. Garofalakis, Ground temperature estimations using simplified analytical and semi-empirical approaches, Solar Energy, 83 (2009) 211-219.
29. T.T. Chow, H. Long, H.Y. Mok, K.W. Li, Estimation of soil temperature profile in Hong Kong from climatic variables, Energy and Buildings, 43 (2011) 3568-3575.
30. L.A. Richards, Capillary conduction of liquids through porous mediums, Physics, 1 (1931) 318–333.
31. R.G. Gonzalez, A. Verhoef, P.L. Vidale, B. Main, G. Gan, Y. Wu, Interactions between the physical soil environment and a horizontal ground coupled heat pump, for a domestic site in the UK, Renewable Energy, 44 (2012) 141-153.
32. G. Gan, Dynamic thermal performance of horizontal ground source heat pumps – The impact of coupled heat and moisture transfer, Energy, 152 (2018) 877–887.
33. G. Gan, Dynamic thermal modelling of horizontal ground source heat pumps, International Journal of Low Carbon Technologies, 8 (2013) 95-105.
34. R. Srivastava, T-C. J. Yeh, Analytical solutions for one-dimensional, transient infiltration toward the water table in homogeneous and layered soil, Water Resources Research 27 (1991) 753-762.
35. F. Stauffer, P. Bayer, P. Blum, N.M. Giraldo, W. Kinzelbach, Thermal use of shallow groundwater, CRC Press, Boca Raton, 2014.
36. G. Gan, Simulation of dynamic interactions of the earth-air heat exchanger with soil and atmosphere for preheating of ventilation air, Applied Energy, 158 (2015) 118-132.

Declarations of interest: none

Figure caption

Fig. 1 Vertical moisture profiles in loam soil for different water table depths (wtd)

Fig. 2 Boundary conditions for simulation of coupled HMT

Fig. 3 Predicted variation of moisture profile from initial setting

Fig. 4 Predicted moisture profiles for the 2nd year and changes from the 1st year
- (a) Predicted variation of moisture profile for the 2nd year
- (b) Change between the 1st and 2nd years

Fig. 5 Effect of initial water table depth on the predicted moisture profile
- (a) Predicted variation of moisture profile with 5 m initial water table depth
- (b) Difference between 5 m and 20 m depths of initial water table

(e) With a uniform moisture content of 0.2 m^3/m^3
(f) With a uniform moisture content of 0.32 m^3/m^3
(g) With a uniform moisture content for each set of conditions
(h) With initial moisture profiles

Fig. 21 Initial moisture content and thermal diffusivity for five types of soil
(c) Moisture content
(d) Thermal diffusivity

Fig. 22 Predicted monthly heat extraction at three installation depths in five soil types
(e) Clay soil
(f) Clay loam soil
(g) Loam soil
(h) Loamy sand soil
(i) Sandy soil

Fig. 23 Predicted total heat extraction at different installation depths in different soil types
(c) Total heat extraction
(d) Increase over clay soil

Fig. 24 Predicted soil temperatures at different installation depths and operating times
(a) Temperature profile and predicted temperature at different times with GHX at 1.5 m deep
(b) Soil temperature with GHX at three depths at the beginning of January
(c) Soil temperature with GHX at three depths at the end of March

Highlights

- A methodology to generate soil moisture and temperature profiles
- Spatiotemporal variation of soil properties
- Coupled heat and moisture transfer in soil-ground heat exchanger system
- Significant impact of soil moisture on thermal performance of ground heat exchanger
- Influence of atmospheric conditions and soil texture